Molecular Therapy
Nucleic Acids
Original Article

Restoring hematopoietic stem and progenitor cell function in *Fancc*$^{-/-}$ mice by *in situ* delivery of RNA lipid nanoparticles

Omar Banda,[1,5] Sarah E. Adams,[2] Linah Omer,[2,3] Seul K. Jung,[2] Hooda Said,[6] Theerapat Phoka,[1,3] Ying Tam,[7] Drew Weissman,[3,5] Stefano Rivella,[3,4,5] Mohamad-Gabriel Alameh,[1,3,5] and Peter Kurre[2,3]

[1]Department of Pathology and Laboratory Medicine, Children's Hospital of Philadelphia, Philadelphia, PA 19104, USA; [2]Comprehensive Bone Marrow Failure Center, Children's Hospital of Philadelphia, Philadelphia, PA 19104, USA; [3]Perelman School of Medicine, University of Pennsylvania, Philadelphia, PA 19104, USA; [4]Department of Pediatrics, Division of Hematology, Children's Hospital of Philadelphia, Philadelphia, PA 19104, USA; [5]Penn Institute for RNA Innovation, University of Pennsylvania, Philadelphia, PA 19104, USA; [6]Department of Bioengineering, George Mason University, Fairfax, VA 22030, USA; [7]Acuitas Therapeutics, Vancouver, BC, Canada

Fanconi anemia (FA) is a congenital multisystem disorder characterized by early-onset bone marrow failure (BMF) and cancer susceptibility. While *ex vivo* gene addition and repair therapies are being considered as treatment options, depleted hematopoietic stem cell (HSC) pools, poor HSC mobilization, compromised survival during *ex vivo* transduction, and increased sensitivity to conventional conditioning strategies limit eligibility for FA patients to receive gene therapies. As an alternative approach, we explored *in vivo* protein replacement by mRNA delivery via lipid nanoparticles (LNPs). Our study aims to address several key obstacles to current mRNA-LNP treatment: access to the HSC niche, effective expression half-life, and potential mRNA LNP immunogenicity. Results demonstrate efficient *in vivo* LNP transfection of murine BM via intravenous or intrafemoral injections, yielding reporter expression across hematopoietic and non-hematopoietic BM niche populations. Functionally, LNP delivery of modified *Fancc* mRNA restored *ex vivo* expansion. In a proof of principle approach, LNP-treated murine *Fancc*$^{-/-}$ HSPCs engrafted with restored alkylator resistance up to 120 h post-treatment using circularized mRNA constructs. *In vitro* delivery of mRNA LNPs resulted in modest differences in innate immune target gene expression in both FA and wild-type HSPCs. Our results suggest that mRNA-LNP-based protein replacement therapy holds promise for clinical translation.

INTRODUCTION

Fanconi anemia (FA) is a congenital hematologic disease characterized by the early onset of bone marrow (BM) failure as well as an elevated predisposition to cancer, especially leukemia.[1,2] To date, deleterious mutations in 22 genes have been definitively linked to the disorder.[3,4] One common role of FA proteins encoded by these genes is the repair of DNA interstrand crosslinks. Loss of FA gene function also leads to the rapid depletion of hematopoietic stem cells (HSCs) and symptomatic BM failure in most patients.[5] The only curative treatment is allogeneic BM transplant, albeit with demonstrated barriers in securing human leukocyte antigen-matched donors and inherent risks to the patient.[6] These risks can be further compounded by secondary malignancies associated with pre-transplant conditioning. Thus, gene repair or addition therapies are attractive alternatives to explore.

Existing approaches to gene therapy for FA focus on restoring protein expression in multipotent HSC populations to preempt BM failure. *Ex vivo* lentiviral transduction of HSCs has demonstrated persistent gene marking and restoration of mitomycin C (MMC) tolerance in hematopoietic progenitor populations in several phase 1/2 pilot studies, but do not show definitive improvement in hematopoietic function.[7,8] These studies have been critical, however, in identifying remaining barriers to clinical success. For example, the need to mobilize HSCs to the peripheral blood for apheresis and *ex vivo* gene transfer leaves adolescent patients with *a priori* reduced HSC pools ineligible for trial enrollment.[8] Conceptually, *in situ* delivery of nucleic acids might overcome these barriers and avoid the loss of HSC engraftment potential due to *ex vivo* culture and improve treatment efficacy.[9–12] Direct *in vivo* delivery also removes the need for the complex infrastructure and logistics associated with *ex vivo* modification, potentially leading to improved accessibility and cost-effective treatment options.[13]

Recent clinical trials for the treatment of monogenic metabolic diseases, including methylmalonic acidemia, acute intermittent porphyria, and ornithine transcarbamylase deficiency, have demonstrated the possibility of chronic *in vivo* replacement by messenger RNA (mRNA) delivered by lipid nanoparticles (LNP^{mRNA}).[14] While this approach

Received 14 June 2024; accepted 10 December 2024;
https://doi.org/10.1016/j.omtn.2024.102423.

Correspondence: Peter Kurre, Comprehensive Bone Marrow Failure Center, Children's Hospital of Philadelphia, Philadelphia, PA 19104, USA
E-mail: kurrep@chop.edu

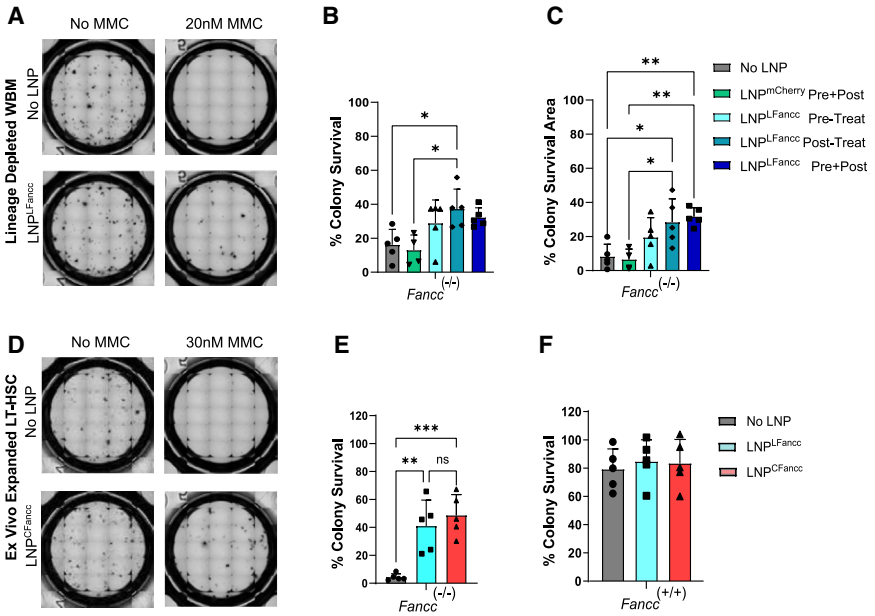

Figure 1. *In vitro* delivery of FANCC LNPs to correct FA-deficient BM-derived HSPCs

(A) Transmitted images of Lin$^-$ whole bone marrow (BM) from Fancc$^{-/-}$ mutant mice in methylcellulose media after treatment with LNP and 20 nM mitomycin C (MMC). (B) Colony survival rates expressed as a percentage ratio of the number of colonies formed after exposure to MMC and of colonies formed without MMC treatment across a range of treatments. (C) Percentage ratios of the sum of colony spread area of colonies in (B). (D) Transmitted images of *ex vivo* expanded LT-HSCs from Fancc$^{-/-}$ mice in methylcellulose media after treatment with LNP and 30 nM MMC. (E and F) Colony survival rates of Fancc$^{-/-}$ or WT *ex vivo* expanded LT-HSCs after pre-treatment with 30 nM MMC and LNP^{LFancc} or LNP^{CFancc}. Data points represent biological replicates ($p < 0.05$).

exploits the tendency of systemically delivered LNP^{mRNA} for sequestration in organs of high blood perfusion such as the liver, efficient transfection and mRNA expression have also been achieved in other tissues.[15–20] These observations suggest that LNP-mediated delivery of mRNA for monogenic disorders may hold clinical utility more broadly. In the context of FA, mRNA delivery to HSCs may offer rescue of hematopoietic function and could support existing gene addition approaches for long-term correction.

Here, we set out to determine whether mRNA LNP can improve outcomes of HSCs in the context of FA. Our studies demonstrate that LNPs efficiently transfect murine BM HSCs *in situ*, after either intravenous (IV) or intrafemoral (IF) injection of LNPs. Additionally, LNP^{Fancc} delivery restored hallmark functions of FA hematopoietic stem and progenitor cells (HSPCs) in a murine FANCC-deficient model (*Fancc*$^{-/-}$) both *in vitro* and *in vivo*, supporting further development of this approach for potential clinical applications in FA patients.

RESULTS

LNP^{Fancc} restores alkylator resistance in *Fancc*$^{-/-}$ HSPCs

Whereas the physiologic triggers for loss of FA HSC remain to be defined, cellular sensitivity of FA cells to bifunctional alkylating agents such as MMC has been a mainstay of diagnosis, and its reversal is considered evidence of correction. Before producing *Fancc* mRNA to formulate LNP^{Fancc}, we first validated a candidate FANCC protein sequence by conferring MMC tolerance to *Fancc*-deficient murine cells using lentiviral vectors to deliver a constitutively expressed *Fancc* transgene. *Fancc*$^{-/-}$ Lin$^-$ (CD3ε$^-$, Ly-6G/Ly-6C$^-$, CD11b$^-$, B220$^-$, TER-119$^-$), Sca1$^+$, c-kit$^+$ (LSK)-expressing cells in mice include the HSPC populations that are orthologs to HSPC populations exhausted by FA in humans. Like their human counterparts, murine *Fancc*$^{-/-}$ LSKs display high sensitivity to alkylating agents. LSKs receiving the *Fancc* transgene via lentiviral transduction displayed similar tolerance to MMC exposure as wild-type (WT) cells in a colony-forming assay, while untreated deficient cells did not proliferate or form colonies (Figure S1). Next, the FANCC mRNA sequence was codon optimized to decrease immunogenicity and improve mRNA yields, quality, and protein expression. The sequence was cloned into a custom *in vitro* transcription template for either linear or circular mRNA production prior to formulation into LNP (LNP^{LFancc} or LNP^{CFancc}). To verify FA pathway restoration in murine *Fancc*$^{-/-}$ cells by LNP, we challenged primary BM enriched for *Fancc*$^{-/-}$ Lin$^-$ populations with MMC after *in vitro* administration of LNP^{Fancc}. LNP treatment improved survival after 24 h of 20 nM MMC exposure by more than 2× (37.2% ± 11%) compared to the untreated cells (16% ± 9.1%) (Figures 1A–1C). Next, we isolated and expanded *ex vivo* cultures of LSKs, enriched for CD150$^+$, CD48$^-$ signaling lymphocytic activation molecule (SLAM) immunophenotype, from normal and *Fancc*$^{-/-}$ mutant mice. These HSC populations typically serve as naive stem cell reserves in the BM and provide long-term (LT) broad repopulation capabilities in the BM. Gradual exhaustion of LT-HSC reserves drives FA disease progression toward BM failure.[21] Pre-treatment with LNP^{LFancc} increased survival rates of MMC-treated *Fancc*$^{-/-}$ HSCs up to 41% ± 18.5% of MMC-free controls, while LNP^{CFancc} increased survival rates up to 48.7% ± 14.8% (Figures 1D–1F). Together, these experiments demonstrate the efficient recovery of MMC tolerance by transient expression of codon-optimized *Fancc* mRNA.

In situ delivery of LNP to the BM broadly transfects BM populations

To develop an *in situ* strategy for FA protein replacement through mRNA delivery, we first sought to characterize LNP delivery to BM hematopoietic cells, comparing systemic IV injection with direct delivery of LNP to IF injection into the medullary space. For these studies, we delivered 3 μg mRNA-LNP encoding the Cre recombinase (LNP^{Cre}) to

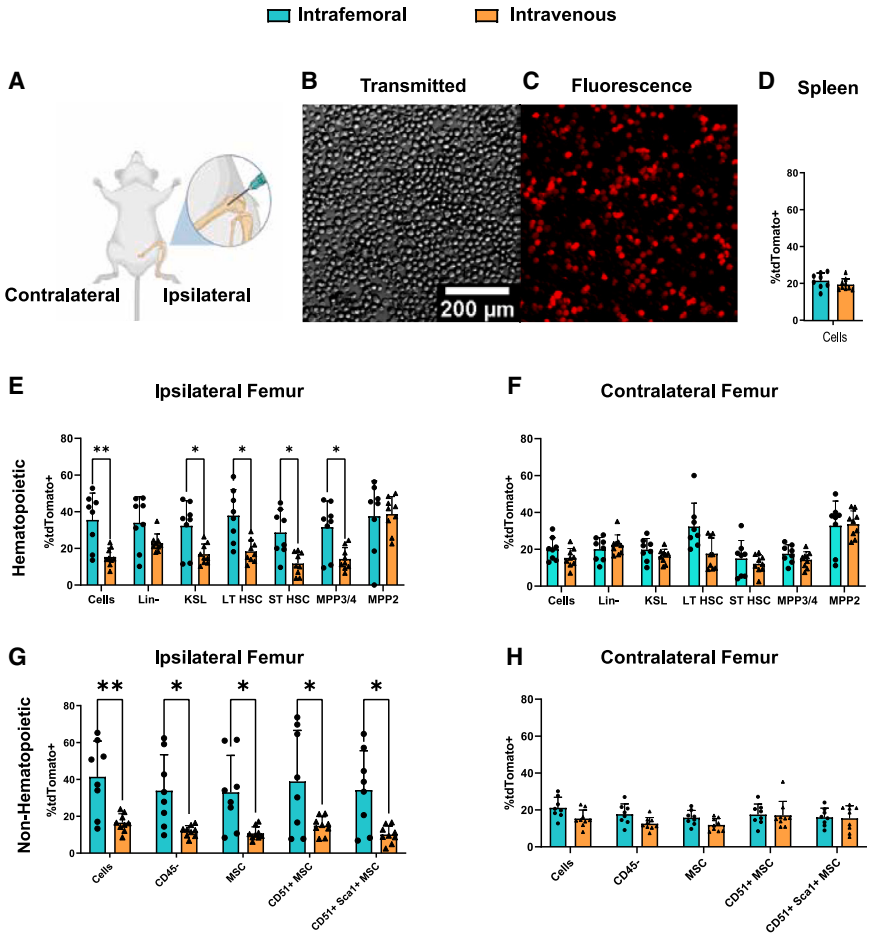

Figure 2. IF delivery of Cre-recombinase LNP to stably induce reporter expression

(A) Graphical representation highlighting the IF injection procedure for delivering LNP directly into the BM. (B and C) Widefield transmitted (B) and fluorescence (C) images of whole BM taken from Ai14 mice after IF LNP^{Cre} delivery. (D–H) FACS analysis of cells from IF- or IV-treated spleens (D) or femurs (E–H) comparing positivity rates between mice treated either IF or IV with LNP^{Cre} ($p < 0.05$).

the tdTomato Ai14 reporter mouse line[22] and measured transfection efficiency in SLAM immunophenotyped populations. These populations include partially committed multipotent progenitors (MPPs), such as MPP2 (LSK, $CD48^+$, $CD150^+$), MPP3 and MPP4 (LSK, $CD48^+$, $CD150^-$), and both LT and short-term naive HSCs (LSK, $CD48^-$, $CD150^+$ and LSK, $CD48^-$, and $CD150^-$, respectively) (Figure 2). Cells from injected femurs displayed increased tdTomato positivity compared to IV-injected mice. However, expression in contralateral (i.e., uninjected) femurs and spleens, representing systemic dissemination, did not change between modes of delivery (Figures 2D–2F). Transfection efficiency within IF or IV delivery did not appreciably differ between different progenitor cell populations. We also collected and analyzed residual non-hematopoietic populations ($CD45^-$, $Ter119^-$) (Figures 2G and 2H) from collagenase digested femurs. Expression of tdTomato in cells of non-hematopoietic origin, such as endothelial cells ($CD31^+$) and mesenchymal stem (MSC) and progenitor cell populations ($CD31^-$, $CD51^{(+\text{ or }-)}$, $Sca\text{-}1^{(+\text{ or }-)}$), closely resembled that of hematopoietic populations, suggesting broad transfection across relevant BM niche cell populations.

Next, we tested a transient reporter system using $LNP^{mCherry}$ to resolve differences in relative LNP uptake per cell based on reporter fluorescence intensity. We compared reporter mean fluorescence intensity (MFI) and positivity rates of both IV- and IF-delivered mCherry mRNA in injected femurs, contralateral femurs (or corresponding femurs in IV administration), and the spleen (Figures 3A–3F). Fluorescence positivity thresholds for mCherry expression were set at the intensity value representing $\leq$0.5% of the positivity rate of untreated samples. In mice receiving IF injections, ipsilateral mCherry expression was significantly increased compared to the contralateral femurs in HSPCs, as well as terminally differentiated populations. Among specific HSPC populations, the proportion of mCherry-expressing cells did not vary between assayed whole BM or SLAM-expressing HSPC populations, suggesting similar transfection efficiencies across all measured cell types in the marrow compartment. In addition, HSPCs from the ipsilateral IF injection demonstrated significantly increased reporter expression (by both positivity rate and MFI) over HSPCs from the corresponding femurs in IV-treated mice (Figures 3A–3D). Contralateral femurs and spleens did not differ in expression between IF- and IV-treated mice (Figures 3B, 3C, 3E, and 3F). To determine whether gains in mCherry fluorescence resulted from increased uptake of LNP^{mRNA}, we performed quantitative real-time PCR analysis to quantify those differences. Consistent with mCherry expression by fluorescence-activated cell sorting (FACS) analysis, relative mRNA transcript levels were also increased in injected femurs (Figures 3G–3I). Unlike the increase in injected femurs, mRNA levels of mCherry transcript in the spleen and contralateral femurs did not differ between IF- and IV-treated mice. We found that both reporter fluorescence and mRNA concentrations of BM populations from injected femurs reached levels found in the spleen, which is known to sequester LNPs in circulation.[23–25]

Next, we administered 10 μg firefly luciferase (FLuc) linear mRNA in LNPs (LNP^{LFluc}) to further resolve organ-level tropism differences between IF and IV modes of delivery by luciferase activity. After 24 h, luciferin was administered intraperitoneally, animals were sacrificed, organs of interest were explanted, and the radiance of individual

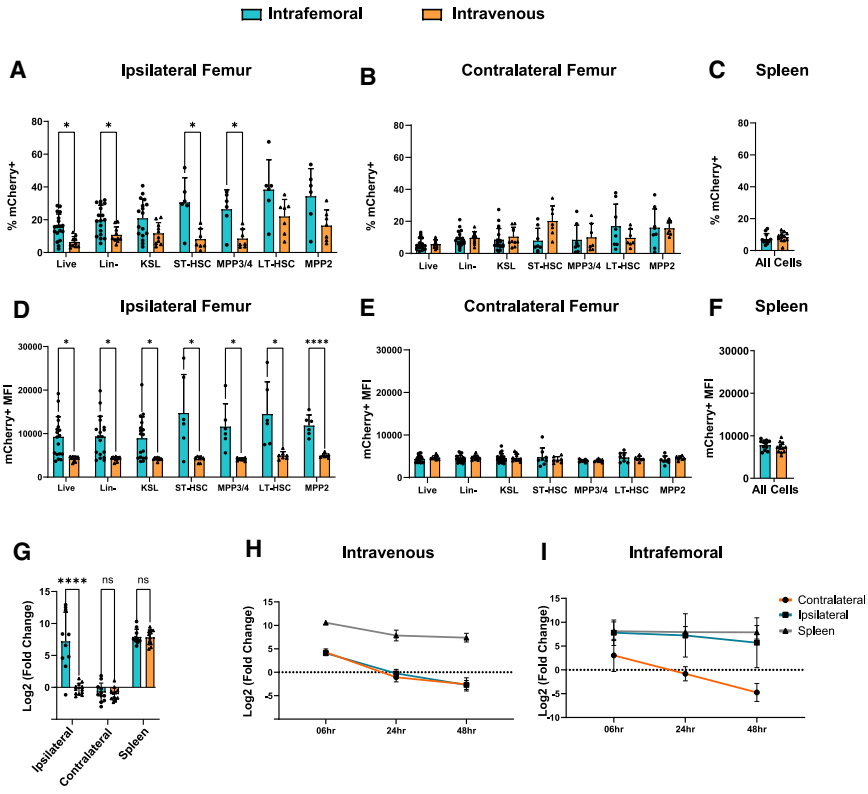

Figure 3. IF vs. IV delivery of fluorescent reporter LNP

Comparisons of mCherry positivity rates (A–C) or mean fluorescence intensity (MFI; D–F) 24 h after either IF or IV delivery of mCherry LNP. (G) quantitative real-time PCR analysis of mCherry RNA isolated from whole BM 24 h post-injection. (H and I) Time series plots of relative mRNA concentrations in the femurs and spleen of IV-treated mice (H) or IF-treated mice (I). All mRNA concentrations are represented as the binary log of the relative fold change from femurs in IV-treated mice ($p < 0.05$).

extracted organs was measured. Consistent with fluorescence data, we observed elevated radiance specifically within injected femurs as compared to the contralateral counterparts. IV injection, by contrast, provided balanced luciferase signal between the two femurs (Figures 4A, 4B, and 4E–4H). A modest gain in fluorescence signals was seen in liver and spleen after IV injection, but differences in radiance between IF and IV delivery in any other organs did not reach significance (Figures 4C, 4D, 4I, and 4J). No differences between modes of injection were seen in biodistribution to heart, lungs, and kidneys (Figure S2).

Expression lifetime of mRNA *in vitro* and *in vivo* is increased by circularization

One natural limitation of mRNA-based protein replacement therapeutics is the limited half-life of mRNA both *in vitro* and *in vivo*. To evaluate the expression lifetime of our mRNA constructs, we performed IF injections of $LNP^{mCherry}$ and measured reporter expression over time in BM populations. Mice were sacrificed at serial time points between 4 and 72 h post-injection, and harvested cell fractions were immunophenotyped (LSK, SLAM) and analyzed by flow cytometry (Figures 5A–5D). Expression of mCherry peaked between 6 and 24 h post-injection in all measured tissues (ipsilateral femur, contralateral femur, and spleen) and was detectable at least 72 h post-injection. In the context of FA, improving the lifetime of mRNA expression *in vivo* could provide a therapeutic bridge during *ex vivo* HSC manipulation. To that end, circular mRNA has previously been reported to maintain a longer *in situ* half-life due in part to the absence of a 5′ cap structure and 3′ poly-adenylated tails, bypassing enzymatic cleavage by endogenous exonucleases.[26,27] To determine whether expression lifetime could be increased within hematopoietic cells using circularized constructs, we next formulated LNPs to deliver FLuc mRNA to *ex vivo* primary cultures as either a linear or circular mRNA construct (LNP^{LFLuc} or LNP^{CFLuc}, respectively). Compared with the mCherry reporter, luciferase enables improved sensitivity for measuring the impact of LNP dose and mRNA expression duration based on the total luminescence of luciferase activity. Consistent with previous reports demonstrating the increased expression lifetime of circular mRNA,[28] we achieved longer luciferase expression lifetimes with LNP^{CFLuc} in both *ex vivo* expanded LT-HSCs and primary mouse embryonic fibroblasts (MEFs) compared to LNP^{LFLuc} (Figures 5E and 5F). When treated with LNPs for 24 h *in vitro*, the peak expression of cells treated with LNP^{CFLuc} occurs at approximately 48- h post-exposure, while LNP^{LFLuc}-treated cells peak shortly after LNP are cleared via media change (t = ∼24 h). In addition, we found that peak expression time and magnitude in these populations can be increased by extending cell-LNP exposure time (Figure S3), suggesting that the rate of particle uptake may be a rate-limiting factor of expression. To confirm the benefits of circularized mRNA *Fancc* constructs, we performed functional lifetime assessments of LNP^{LFancc} and LNP^{CFancc}. We measured survival rates of LNP-treated *Fancc* mutant *ex vivo* expanded LT-HSCs as a function of MMC exposure time (Figures 5G and 5H). *Fancc*-deficient *ex vivo* expanded HSCs exposed to 30 nM MMC for at least 24 h do not proliferate and will undergo apoptosis by day 6. In contrast, cells pre-treated with LNP^{LFancc} or LNP^{CFancc} for 24 h prior to MMC exposure both display varying levels of improved tolerance relative to WT cells for up to 48 h of total MMC exposure. LNP^{CFancc} additionally displays significantly increased relative survival for up to 96 h of MMC exposure, suggesting a conferred MMC tolerance of up to 5 days post-LNP treatment (Figure 5H).

LNPs are not potent immune activators of HSPCs

FA hematopoietic cells are particularly vulnerable to quiescence loss, DNA damage accumulation, and inflammation exhaustion.[29–31] To

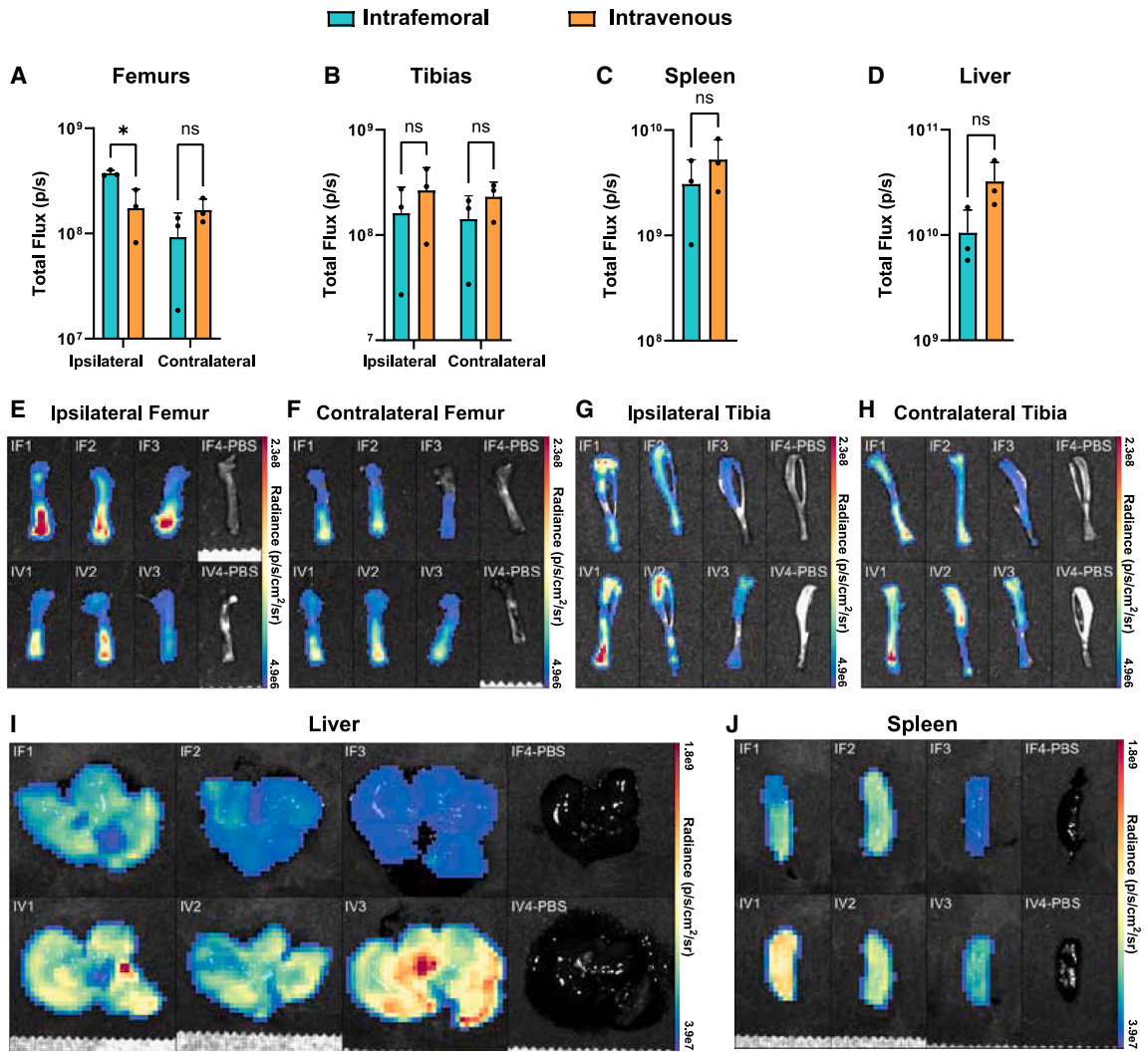

Figure 4. *In vivo* LNP^{LFluc} expression after IF or IV delivery

(A–D) Graphs of the total luminescent flux measured after D-luciferin administration in LNP^{LFluc}-treated mice. (E–J) Heatmaps of radiance from organs, corresponding to those in (A)–(D), reveal the distribution of radiance displayed as an overlay on reflected light images of the respective organ.

investigate the impact of LNPs, which can be broadly inflammatory,[32,33] on *Fancc*$^{-/-}$ HSCs, we initially screened WT and *Fancc*$^{-/-}$ *ex vivo* expanded LT-HSCs by array-based quantitative real-time PCR. Expression of innate and adaptive immune response genes was assayed after 6 or 24 h of exposure to 8.3 μg LNP^{LFancc} or LNP^{CFancc} per million cells and compared with respective untreated controls (Figure S4). In the context of LNP treatment, selective regulation of immunomodulatory genes was observed. Of the 84 genes screened, 15 genes in LNP^{LFancc}-treated and 23 genes in LNP^{CFancc}-treated cells were differentially expressed by a factor of at least 1.5 in both WT and mutant cells. To determine whether the *ex vivo* expanded populations were representative of inflammatory signaling *in vivo*, we next screened freshly isolated KSL populations from either WT or knockout (KO) mice treated with LNP^{CFancc} *in vitro* for 24 h (Figure 6A). In the pooled KSL populations, baseline differences in expression between WT and KO were evidenced by a mild increase in inflammatory signaling in the mutant *Fancc* population. For validation, replicate tests in these populations were performed by assaying the most prominently differentially expressed genes by quantitative real-time PCR. Overall, while the trend of increased inflammation in KO populations held, we did not find consistent significant differences in expression between genotypes or between LNP treatment groups (Figures 6B and S5).

Repeat dosing of LNP^{CFancc} increases HSPC clonogenicity *in vitro*

While MMC resistance faithfully represents the activity of FA proteins in DNA repair, we were looking for an improved metric of HSPC function unprovoked by alkylating agents or other experimental challenges. We showed that the duration of expression after

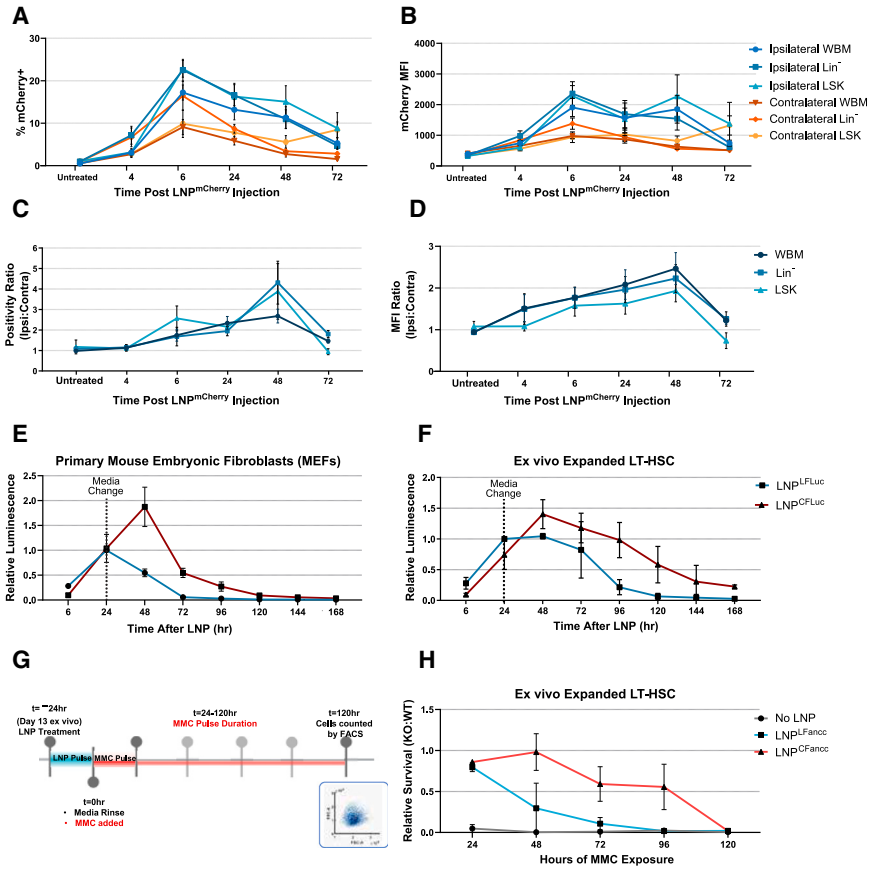

Figure 5. Functional lifetime of LNP mRNAs

(A and B) Time series plots of positivity rates (A) or MFI (B) after $LNP^{mCherry}$ IF delivery measured up to 72 h post-injection. (C and D) Time series plots of luminescence as a function of time post-exposure to either linear or circular luciferase mRNA delivered with LNP in *ex vivo* expanded HSCs (C) or MEFs (D). (E) Graphical representation of the methodology employed to determine the functional lifetime of LNP^{LFancc} and LNP^{CFancc}. Briefly, *ex vivo* expanded cells were treated with LNP for 24 h, prior to a media change and addition of 30 nM MMC. (F) Relative survival, expressed as a ratio between FA and WT cells of the relative survival with and without MMC exposure, is plotted as a function of total exposure time to MMC over a 6-day period post-LNP treatment ($p < 0.05$). (G) Experimental schema for scoring MMC tolerance and survival of LT-HSC following a single LNP treatment. (H) Survival advantage of *ex vivo* expanded LT-HSC treated with LNP carrying circular Fancc mRNA.

a single dose of LNP^{CFancc} is insufficient to show differences in progenitor clonogenicity between mutant and WT populations. Therefore, to determine whether the *Fancc* mutant deficit in clonogenicity could be improved by LNP^{CFancc}, we explored the effects of repeat dosing of LNP^{CFancc} *in vitro*. LT-HSCs isolated from *Fancc* mutant and WTmice were expanded over 14 days, and LNP^{CFancc} was administered on days 0, 7, and 14 post-isolation. The total population doublings as a function of time were obtained from raw cell counts (Figure 7A). We found that multiple doses of LNP^{CFancc} significantly improved proliferation and, additionally, brought the number of doublings in mutant HSCs up to that of the WT controls over a 14-day period. This contrasts with mutant *Fancc* LT-HSCs treated with a single dose of LNPs, which did not show significantly improved doubling over untreated controls (Figure S6). Next, expanded cells were treated with varying concentrations of MMC at day 15 of *ex vivo* culture for 24 h prior to plating into a colony-forming unit (CFU) assay at 500 cells/well (Figures 7B and 7C). When colonies were counted at day 7 post-plating, *ex vivo* LNP^{CFancc} primed KO populations revealed an increase in colony counts and relative survival compared to untreated controls at both 10 and 100 nM MMC treatments. Additionally, expanded LT-HSCs were immunophenotyped to assess the relative proportions of HSPC populations (Figure 7D). *Fancc* mutant mice treated with LNP^{CFancc} exhibited an increased proportion of stem cells retaining LT-HSC immunophenotyping relative untreated cells, and no difference was observed compared to WT mice.

Ex vivo treatment of *Fancc*$^{-/-}$ LT-HSC improves engraftment potential

Fancc$^{-/-}$ HSCs display reduced proliferation rates and decreased engraftment potential relative to their WT counterparts. To determine the impact of temporary restoration of the FA pathway on HSC behavior, we performed comparative studies of *ex vivo* expanded HSCs after treatment with *Fancc* mRNA LNP. When transplanted into lethally irradiated recipients in a competitive transplant setting, *ex vivo* expanded *Fancc*$^{-/-}$ LT-HSCs display decreased engraftment potential relative to WT controls based on day 14 donor chimerism post-transplant. Treatment with LNP^{CFancc} prior to transplantation did not alter performance at this time point (Figure 7E), except when cells were first challenged by exposure to MMC for 6 h prior to transplantation. After MMC challenge, untreated *Fancc*$^{-/-}$ LT-HSCs displayed greatly diminished engraftment potential. Remarkably, this loss is completely protected against by pre-treatment selection using LNP^{CFancc}. These data identify LNP treatment as a potential adjuvant therapeutic during *ex vivo* manipulation of *Fancc*$^{-/-}$ HSPCs.

DISCUSSION

Ex vivo modification of HSPC in FA patients has provided strong proof of principle for the potential of protein replacement by lentiviral gene addition. However, definitive hematologic improvement remains to be shown, potentially owing to oligoclonal reconstitution with corrected stem cells.[34] Studies in metabolic disorders suggest that *in vivo* delivery of modified mRNA using a non-viral approach may be an alternative treatment approach that relies on repeat dosing. Our studies lay out basic observations on key variables of LNP

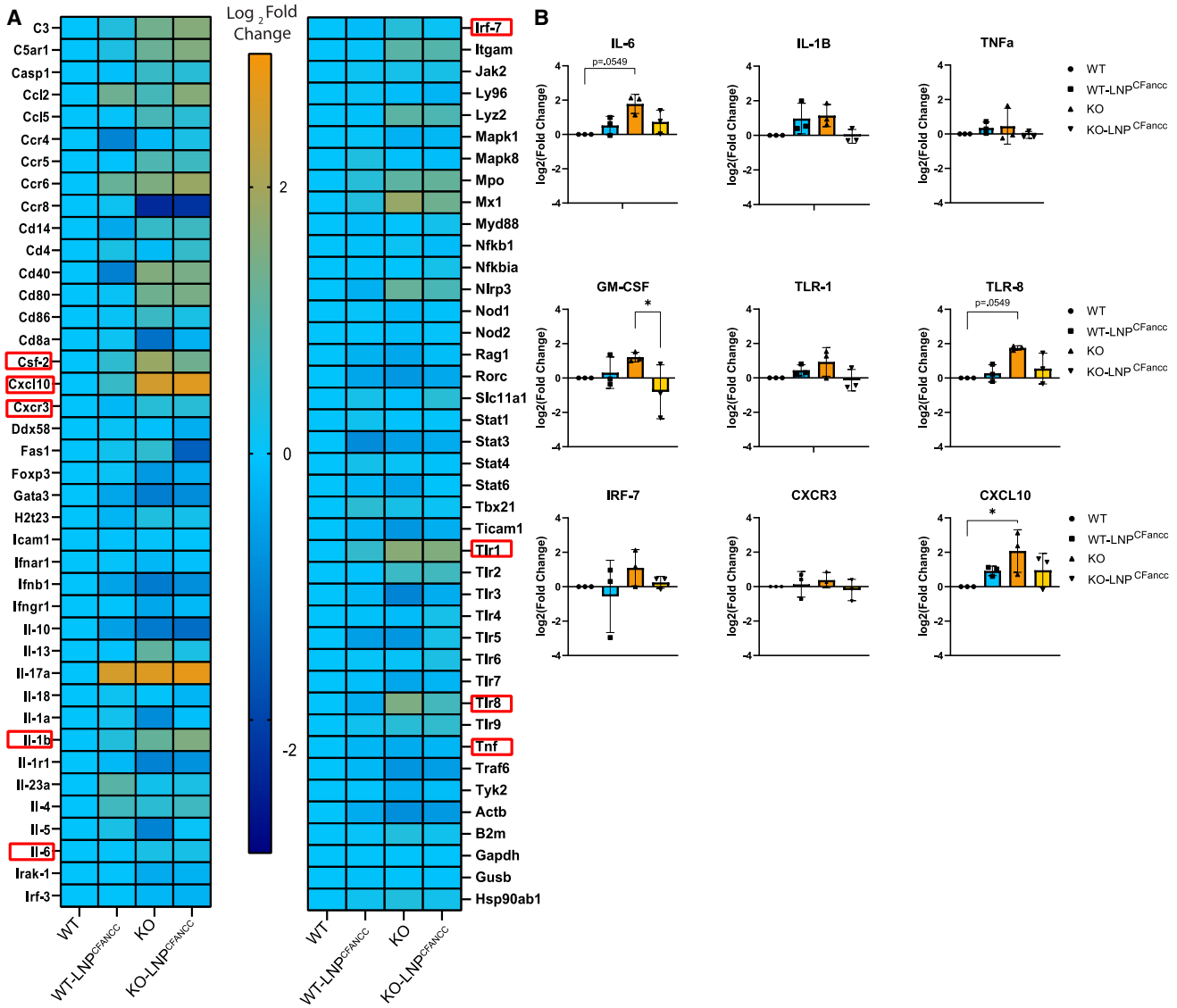

Figure 6. Immune screening of HSPCs after LNP treatment

(A) KSL populations were pooled from three mice and screened for 84 innate and adaptive immune markers by quantitative real-time PCR array 24 h after treatment with LNP^{CFancc}. Values are expressed as the binary logarithm of the fold change difference to the expression of the untreated WT population. (B) Nine targets representing either elevated expression in the screening array or commonly assayed targets in the context of LNP immunogenicity were analyzed in replicate ($p < 0.05$).

delivery, durability, and immunogenicity toward that goal and demonstrate promise for LNP treatment in FA.

To this end, we delivered LNPs IF and IV to determine the efficiency of delivery to HSPCs in the BM. Consistent with other reports employing systemic LNP delivery,[15,20] we observe dose-dependent transfection efficiency, with high rates of transfection in a Cre-sensitive tdTomato reporter mouse model. Side-by-side comparisons of systemic and direct delivery modes highlight the decreased access to BM after systemic delivery, which is increased to levels found in the spleen by directly injecting LNP into the medullary space. These data suggest that low transfection efficiency by systemic delivery in the BM is primarily the product of decreased physical access to BM cells through normal blood circulation. This decrease is likely due to systemic dissemination of LNPs to organs of high blood perfusion such as the spleen, liver, and lungs, decreasing the effective concentration of LNPs reaching the BM and resulting in diminished transfection. Therefore, direct delivery to the BM might increase transfection efficiency through bypassing LNP loss in circulation prior to arrival in the BM. Interestingly, our data demonstrate that LNPs delivered IF achieve similar levels of expression in typically high-expressing tissues in systemic delivery models, suggesting that elevated initial

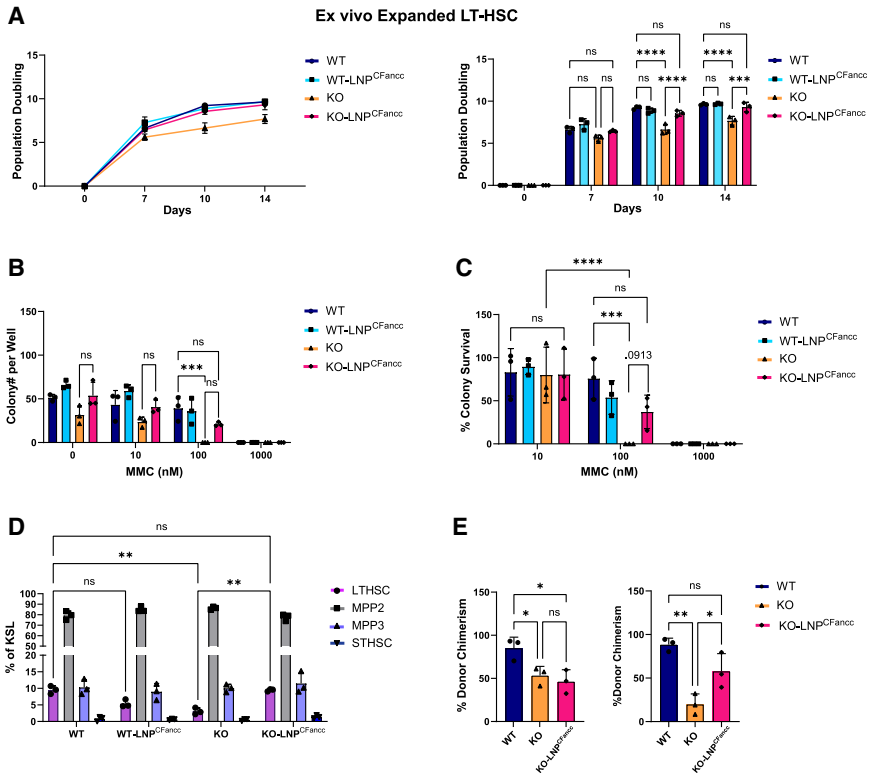

Figure 7. Impact of LNP^{CFancc} on Fancc$^{-/-}$ HSPC *in vitro* proliferation and engraftment potential

(A) LT-HSCs isolated from WT or Fancc$^{-/-}$ mice were treated on days 0, 7, and 14 of *ex vivo* culture with LNP^{CFancc}. Shown are population doublings calculated from cell counts at days 0, 7, 10, and 14. (B) After 15 days of *ex vivo* expansion, cells were incubated with MMC for 24 h prior to plating in CFU assay. Colonies were counted at 7 days post-plating. (C) Colony survival was determined as the number of colonies at a given condition relative to the respective cell population in MMC-free methylcellulose media. (D) LT-HSC populations were immunophenotyped and analyzed by FACS to determine relative proportions of HSPC subpopulations after 15 days of *ex vivo* expansion. (E) *Ex vivo* expanded LT-HSCs receiving a single dose of LNP^{CFancc} at day 14 for 24 h were transplanted into lethally irradiated recipient mice either with (right) or without (left) 6 h of *in vitro* MMC exposure prior to transplantation.

concentrations are enough to significantly improve local medullary transfection efficiency, despite subsequent systemic dissemination. While direct access to the BM compartment is less common in the clinic than other routes for administration of drug product, the means do exist, offering the potential for reduced hepatotoxicity. In fact, several US Food and Drug Administration-approved devices to simplify access to the BM already exist (e.g., EZ-IO system) and are typically employed to allow vascular access for infusions in the absence of a viable IV route. Recently, mRNA BM transfection efficiency was shown to be increased by targeting LNPs through surface modifications to specifically bind the c-kit receptor (CD117) on HSPCs.[15] A combination of methods may be required to improve access to the HSC niche for maximum impact and to minimize any potentially negative off-target effects.

While HSC defects are a near-uniform feature in FA, dysfunction within BM mesenchymal stroma has also been reported.[35–37] FA BM MSCs demonstrate compromised osteoblast differentiation and decreased bone formation.[35] Additionally, murine BM MSCs display impaired hematopoietic support, as evidenced by decreased homing and engraftment by transplanted HSCs.[37] While it is currently unknown what consequences FA gene correction may have in cells other than BM HSCs, it is possible that mRNA therapies could improve other functional aspects of the BM niche. Using the Cre-reporter system, our data show consistent uptake and expression of mRNA cargo in both hematopoietic and non-hematopoietic immunophenotyped cell populations, including stromal populations such as osteogenic MSCs (CD45^{-},CD31^{-},CD51^{+},Sca1^{+}). This consistent uptake across BM populations suggests that transfection efficiency in our models relies primarily on local LNP concentrations rather than cell-specific interactions or tissue tropism. While the effects of FA complementation in non-hematopoietic cells is unknown, future work will elucidate whether compartment-wide transfection by *Fancc* LNPs in the BM could offer additional benefits.

While viral gene addition provides permanent HSPC correction, mRNA delivery will have transient effects that may require redosing for any durable clinical benefit. In addition, unlike common viral approaches, dosing LNP-mediated mRNA delivery is not known to be limited by adaptive immunoreactivity.[38] Nevertheless, reduced dosing frequency will reduce logistical burdens of treatment. To that end, one existing approach to extend mRNA expression lifetime is by circularization of mRNA constructs. Our results using circularized variants of our FLuc and *Fancc* LNP demonstrated 2–3 days of additional expression by functional assays. Additionally, work in FA and other congenital disorders has demonstrated that select patient mutations may be amenable to LNP-mediated CRISPR-based editing approaches for permanent repair.[15,39,40] Another potential therapeutic modality that we did not explore is the use of self-replicating RNA (srRNA) vectors.[41] These vectors enable longer-term expression of protein products up to 7 weeks.[42] Unfortunately, currently available srRNA backbones are virally derived, and their RNA products tend to elicit immune responses.[43] For this reason, we have not yet explored their use. While the reporter systems employed here are less logistically complex than existing editing approaches, the potential efficiency of such an approach is illustrated by our Cre-based LNP reporter system. We find that an LNP^{Cre} dose of roughly 25% of the magnitude of the LNP^{mCherry} mRNA mass employed in the mCherry experiments (3

vs. 12.5 μg) yields recombination in over 40% of cells, while an equivalent dose of LNP^{Cre} (12.5 μg) yields greater than 90% recombination in LSK BM populations (Figure S7). The apparent differences in reporter positivity as a function of mRNA dosing between the mCherry and Cre experiments highlight that the observed LNP mRNA delivery efficiency to cells is subject to the functional output of the mRNA gene product and likely needs be determined empirically. In the case of fluorescent reporters, for example, observed positivity rates are limited by factors such as mRNA translation rates, reporter lifetime, and detector sensitivity.

In the context of our *Fancc* LNP, one limitation of the *Fancc* mouse model used in these studies is that mutant mice do not naturally present with BM failure. This limitation complicates the faithful modeling of endogenous HSPC rescue by our *Fancc* LNP in restoring function in the BM, compounded by the transient nature of the protective effects we show here. A more robust model of BM failure, along with repeat dosing schemes, will likely be necessary to achieve time-resolved metrics concerning long-term therapeutic effects of LNP-mediated management of FA.

While safety has been demonstrated in *ex vivo* lentiviral modification of HSCs, immune recognition is a natural barrier to using lentiviral vectors *in vivo*.[38] Indeed, lentiviral vectors promote low-level inflammation and can elicit adaptive innate immune responses, but this has not been explored in FA.[44,45] LNPs such as those we present here have also demonstrated innate inflammatory activity; however, our results demonstrate no significant inflammatory responses in HSPCs after exposure to LNPs. Despite this, one common approach for immunosuppression in the context of drug delivery is pre-treatment with broadly immunomodulatory glucocorticoids, such as dexamethasone. Dexamethasone typically suppresses adaptive T cell response signals in the context of LNPs.[46] This approach does not seem to blunt the beneficial LNP^{Fancc} response *in vitro* (Figure S8) and may optimize repeat dosing regimens to extend expression durability beyond that of a single mRNA dose. This or other more specific immunosuppression approaches may prove vital if adaptive immunity is eventually realized as a complication of LNP delivery for protein replacement therapies. Additionally, FA HSCs are known to exist in an elevated inflammatory state, which has been hypothesized to assist in the proliferation of FA HSCs despite cell-cycle blockades by p53/p21 activity. Several of the previously reported inflammatory signals caused by LNPs are known to act upstream of MYC, a strong promoter of proliferative capacity through the activity of downstream effector targets. Our limited studies suggest that LNP treatment of FA HSPC may provoke only a limited innate immune response that is largely similar to what is observed in WT cells. Interestingly, our data suggest a possible trend of decreased immune cytokine expression in FA HSCs based on transcript levels measured by quantitative real-time PCR (Figure 6), although additional studies are required to further qualify this observation.

In aggregate, our results demonstrate that LNP access to the HSC niche can deliver mRNA for protein replacement to restore FA HSPC proliferative capacity and alkylator resistance. This work serves as a first step toward clinical translation and illustrates the successful adaptation of an LNP platform for a congenital blood disorder.

MATERIALS AND METHODS

Materials

A general list of materials and their sources is provided in Table S1.

Animal husbandry

All animal studies were approved by the Children's Hospital of Philadelphia institutional animal care and use committee and performed according to their guidelines. $Fancc^{-/-}$ and WT mice were bred from C57BL/6 FANCC chimeric mice genetically modified to present a single deletion of exon 8 of the FANCC gene, resulting in a downstream frameshift and, therefore, deletion of the C-terminal half of *Fancc*.[47] Mice were housed with up to four littermates with unlimited access to chow. For BM harvests, mice were sacrificed via CO_2 asphyxiation, and the pelvis, femurs, and tibias were isolated from tissue and flushed with Hank's balanced salt solution using a 26G needle. Transplantation of *ex vivo* expanded HSCs was performed on lethally irradiated (two doses of 5.2 Gy 4 h apart) mice by tail vein injection of 100 μL PBS containing 420,000 *ex vivo* expanded cells and 250,000 whole BM cells from healthy C57BL/6 donors. Blood samples were obtained through retro-orbital access in anesthetized mice. Ai14 mice were purchased from The Jackson Laboratory and are a Cre reporter strain presenting a loxP-flanked STOP cassette upstream a tdTomato reporter gene located at the *Gt(ROSA)26Sor* locus.

LNPs

Linear and circular synthetic mRNA constructs were produced with either 5′ CleanCap or IRES sequence, a 101-repeat poly(A) tail, and N1-methylpseudouridine modifications. Circularization was achieved using a *Tetrahymena thermophila* ribozyme-based RNA circularization system. RNA products were purified by size-exclusion chromatography and precipitated before resuspension at 1 mg/mL for use. LNPs (polydispersity index 0.01–0.1, diameter 80 ± 5 nm) were obtained from Acuitas Therapeutics (Vancouver, BC, Canada) and contained a proprietary ionizable cationic lipid/phosphatidylcholine/cholesterol/polyethylene glycol (PEG)-lipid as described in patent application WO2020146805A1, or were produced using the commercially available ionizable lipid SM-102 (Broadpharm), along with helper lipid distearoylphosphatidylcholine (DSPC; Avanti Polar Lipids, AVP), cholesterol (Sigma), and either ALC-0159 (AVP) or DMG-PEG 2000 (AVP). SM-102 LNP used molar ratios of 50:10:38.5:1.5 for SM-102:DSPC:cholesterol:DMG-PEG 2000. After formulation, LNPs were concentrated by spin column and sterile filtered before use. Final RNA content and concentration were determined by Ribogreen assay. The respective formulation used for each experiment is highlighted in Table S2.

LNP injections

LNPs were delivered to mice either IV or IF. IV delivery was performed by diluting stock LNP to a 100-μL volume dose containing up to 12.5 μg mRNA in PBS and administering the dose via tail

vein injection using a 28G insulin syringe. IF delivery was achieved using a 28G insulin syringe to access the medullary space of the left femur axially through the distal end. A custom plastic spacer was used to control injection depth, and up to 20 μL LNP solution was administered manually.

In vivo luciferase expression

C57BL/6 WT mice between 7 and 9 weeks of age were treated by IV or IF injection of 10 μg LNP^{LFluc}. After 24 h, mice were administered 200 μL 16.7 mg/mL D-luciferin substrate solution (Regis Technologies). After a 10-min rest time, mice were sacrificed, and femurs, tibias, liver, spleen, lungs, heart, and kidneys were excised. For each mouse, all organs were imaged simultaneously except for liver and spleen due to their relatively elevated radiance. Mice were processed sequentially to ensure equal luciferin rest times and organ extraction delays prior to imaging by IVIS Spectrum (PerkinElmer) live animal imager. All images were captured within 15 min of sacrificing. Images were processed by custom MATLAB scripts using calibrated values of intensity to radiance relationships.

Cell culture

All *ex vivo* LSK or Lin^- populations were cultured in STEMSPAN media (STEMCELL Technologies) with 10 ng/mL interleukin-3 (IL-3), 10 ng/mL IL-6, and 50 ng/mL stem cell factor (SCF). HSC ($KSL,CD48^-, CD150^+$) populations were expanded in *ex vivo* cultures based on previously reported methods for efficient *ex vivo* expansion.[48] Briefly, sorted HSCs were seeded on human plasma fibronectin (Sigma-Aldrich)-coated 24-well tissue culture plates in F12 medium supplemented with 1 mg/mL polyvinyl alcohol, 0.01 M HEPES, 1% (v/v) 100× penicillin-streptomycin-glutamine (Gibco), 1% (v/v) 100× insulin-transferrin-selenium-ethanolamine (Gibco), 100 ng/mL murine thrombopoietin, and 10 ng/mL murine SCF. Cells were expanded up to 14 days with initial media changes 5–6 days post-seeding and in 3-day intervals afterward. Mouse embryonic fibroblasts were cultured in DMEM with 10% v/v fetal bovine serum and 1% v/v penicillin-streptomycin.

Flow cytometry analysis

For flow cytometric analysis, whole BM was flushed from the femurs using sterile PBS with 1% v/v penicillin/streptomycin. Flushed BM was strained through a 70-μm filter, centrifuged at 400 rcf for 5 min, and resuspended in RBC lysis buffer (BioLegend) diluted to working concentration in deionized water. Cells were washed with PBS, resuspended in immunophenotyping buffer for 20 min (BM: FITC Mouse Lineage Antibody Cocktail, ckit, Sca-1, CD150, CD48; BM niche cells: Ter119, CD45, CD51, CD31, Sca-1), and rinsed again with PBS prior to FACS analysis. All samples were analyzed using a Cytek Aurora spectral analyzer, and spectral data were processed using custom MATLAB scripts. For reporter analyses, positivity thresholds for the mCherry reporter were defined as the intensity value yielding 0.5% positivity in unstained cell populations within each cohort. MFI values are reported as the mean intensity of cells above the positivity threshold.

quantitative real-time PCR

To analyze relative concentrations of exogenous mCherry and *Fancc* mRNA, total RNA was extracted from whole BM or spleen cells (RNeasy Micro Plus Kit, Qiagen), and reverse transcribed (SuperScript IV VILO, Invitrogen). cDNA was either analyzed immediately using real-time PCR (PowerUp SYBR Green Master Mix, Applied Biosystems; ViiA 7 Real-Time PCR System, Thermo Fisher), or stored at −80°C until analysis. Primers were obtained from Harvard PrimerBank unless otherwise specified. Primers for synthetic mRNA constructs mCherry and cotFANCC were custom designed, ordered from Integrated DNA Technologies, and validated before use. RT2 Profiler arrays used for screening immune gene expression were loaded with 4 ng *ex vivo* expanded HSCs per well in SYBR Green Master Mix. Relative mRNA concentrations are approximated by normalization to glyceraldehyde 3-phosphate dehydrogenase within biological replicates, followed by normalization to a common sample and expressed as the binary log of the relative fold change.

Immunofluorescence imaging and foci counting

Mouse embryonic fibroblasts derived from fetal WT and mutant FANCC embryos harvested between embryonic day (E)12 and E14 were seeded at 20,000 cells/well in optically thin F-bottom 96-well plates for 2 days before treatment with LNP, MMC, or both. Four hours after MMC treatment, cells were fixed in 4% paraformaldehyde, permeabilized in PBS with 0.1% v/v Triton X-100 for 15 min, blocked for 1 h in a blocking buffer (5% BSA in PBS-Tween 20 [PBS-T]), and then stained for 1 h with Alexa Fluor 488 anti-γH2AX and Alexa Fluor 647 anti-Fancd2 in PBS-T. Wells were then rinsed three times with PBS-T before incubation in 1 μg/mL DAPI in PBS-T for 5 min before a final PBS-T rinse. Wells were imaged on a Zeiss Axio Observer 7 widefield microscope using a 40× 0.95 numerical aperture air objective operated through the Zen Blue software. Tiled images were taken at the center of each well, with triplicate wells per condition. Foci and nuclei were analyzed in MATLAB using a custom script.

Colony-forming assays

For Lin^- CFUs, whole BM from WT or mutant FANCC mice was flushed and enriched for hematopoietic progenitor cells using EasySep Mouse Hematopoietic Progenitor Cell Isolation Kit (STEMCELL Technologies). Lin^- cells were counted and seeded at 60,000 cells/well in a 48-well non-treated tissue culture plate in STEMSPAN media with growth factors. Cells were then treated with 0.5 μg LNP. At 24 h after LNP treatment, cells were exposed to 20 nM MMC for 24 h before media change and additional 0.5 μg LNP treatment. At 6 h after the second treatment, cells were plated in methylcellulose media at 5,000 cells/mL and cultured for 8 days in a 6-well plate. Colonies were imaged using a STEMvision imager (STEMCELL Technologies) and analyzed in MATLAB using a custom script.

Proliferation assays

Liquid culture assays to probe $Fancc^{-/-}$ survival after MMC treatment in *ex vivo* expanded HSCs were prepared by treating 13-day

expanded LT-HSCs with LNP for 24 h, followed by MMC treatment for 24, 48, 72, 96, or 120 h. Cells remaining in wells 6 days post-LNP treatment were counted via FACS (Cytek Aurora) in 96-well v-bottom plates. Survival was approximated by comparing the number of cells in MMC-treated replicates to the number of cells in MMC-free wells and normalized to the performance of WT cells in the same conditions. For dexamethasone studies, whole BM from WT or mutant FANCC mice was flushed and enriched for hematopoietic progenitor cells using EasySep Mouse Hematopoietic Progenitor Cell Isolation Kit (STEMCELL Technologies). Cells were counted and seeded at 30,000 cells/well in a 48-well non-treated tissue culture plate. For *in vitro* assays, cells were then treated with 0.25 μg LNP. At 24 h after LNP treatment, cells were exposed to 20 nM MMC for 24 h before media change and additional 0.25 μg LNP treatment. Cells were cultured for 5 days and were counted using a DeNovix CellDrop FL automated counter.

Statistical analysis

All statistical analyses and graphs were generated by either GraphPad Prism 9 or MATLAB (R2021a) ($p > 0.05$ for all analyses). In cases where one-way ANOVA was performed and multiple comparisons were performed post-hoc, the Tukey method was employed when comparing all means, and Bonferroni-Dunn was employed when comparing pairs of means. All data used in statistical comparisons were assumed to be homoscedastic and normally distributed.

DATA AND CODE AVAILABILITY

All flow cytometry, quantitative real-time PCR, and imaging raw data are maintained on institutionally managed servers and are available upon request.

ACKNOWLEDGMENTS

This work was funded in part by the Cell & Gene Therapy Collaborative at the Children's Hospital of Philadelphia. L.O. was supported by 5-T32-HL-007150-47 (Poncz/Chou, principal investigators). We thank Dr. Florin Tuluc and Jennifer Murray of the Children's Hospital of Philadelphia Flow Cytometry core facility and Dr. Benjamin Davis and Dr. Houping Ni from the Engineered mRNA and Targeted Nanomedicine core for technical assistance. We thank Danielle Kobulsky for editorial review. Graphical representations were produced using BioRender.

AUTHOR CONTRIBUTIONS

O.B. and P.K. conceptualized the study and experimental design and edited the manuscript. O.B. performed experiments, analyzed data, and wrote the manuscript. S.A. performed experiments, analyzed data, and edited the manuscript. L.O., S.A., S.J., and T.P. assisted in performing experiments. M.-G.A., H.S., and D.W. designed and produced mRNA and formulated and provided mRNA-LNP. Y.T. formulated and provided LNPs. S.R. and M.-G.A. provided insights into the experimental design and findings. All authors read and approved the manuscript.

DECLARATION OF INTERESTS

Y.T., D.W., and M.-G.A. are named on patents that describe LNPs for the delivery of nucleic acid therapeutics, including mRNA, and the use of modified mRNA in LNPs as a vaccine platform.

SUPPLEMENTAL INFORMATION

Supplemental information can be found online at https://doi.org/10.1016/j.omtn.2024.102423.

REFERENCES

1. Kelaidi, C., Makis, A., Petrikkos, L., Antoniadi, K., Selenti, N., Tzotzola, V., Ioannidou, E.D., Tsitsikas, K., Kitra, V., Kalpini-Mavrou, A., et al. (2019). Bone Marrow Failure in Fanconi Anemia: Clinical and Genetic Spectrum in a Cohort of 20 Pediatric Patients. J. Pediatr. Hematol. Oncol. *41*, 612–617. https://doi.org/10.1097/mph.0000000000001549.

2. Bagby, G. (2018). Recent advances in understanding hematopoiesis in Fanconi Anemia. F1000Res. *7*, 105. https://doi.org/10.12688/f1000research.13213.1.

3. Milletti, G., Strocchio, L., Pagliara, D., Girardi, K., Carta, R., Mastronuzzi, A., Locatelli, F., and Nazio, F. (2020). Canonical and Noncanonical Roles of Fanconi Anemia Proteins: Implications in Cancer Predisposition. Cancers *12*, 2684. https://doi.org/10.3390/cancers12092684.

4. Amenábar, J.M., Torres-Pereira, C.C., Tang, K.D., and Punyadeera, C. (2019). Two enemies, one fight: An update of oral cancer in patients with Fanconi anemia. Cancer *125*, 3936–3946. https://doi.org/10.1002/cncr.32435.

5. Hughes, A.D., and Kurre, P. (2022). The impact of clonal diversity and mosaicism on haematopoietic function in Fanconi anaemia. Br. J. Haematol. *196*, 274–287. https://doi.org/10.1111/bjh.17653.

6. Baxter-Lowe, L.A., Maiers, M., Spellman, S.R., Haagenson, M.D., Wang, T., Fernandez-Vina, M., Marsh, S.G.E., Horowitz, M., and Hurley, C.K. (2009). HLA-A disparities illustrate challenges for ranking the impact of HLA mismatches on bone marrow transplant outcomes in the United States. Biol. Blood Marrow Transplant. *15*, 971–981. https://doi.org/10.1016/j.bbmt.2009.04.015.

7. Río, P., Navarro, S., Guenechea, G., Sánchez-Domínguez, R., Lamana, M.L., Yañez, R., Casado, J.A., Mehta, P.A., Pujol, M.R., Surrallés, J., et al. (2017). Engraftment and in vivo proliferation advantage of gene-corrected mobilized CD34(+) cells from Fanconi anemia patients. Blood *130*, 1535–1542. https://doi.org/10.1182/blood-2017-03-774174.

8. Río, P., Navarro, S., Wang, W., Sánchez-Domínguez, R., Pujol, R.M., Segovia, J.C., Bogliolo, M., Merino, E., Wu, N., Salgado, R., et al. (2019). Successful engraftment of gene-corrected hematopoietic stem cells in non-conditioned patients with Fanconi anemia. Nat. Med. *25*, 1396–1401. https://doi.org/10.1038/s41591-019-0550-z.

9. Cappelli, E., Degan, P., Bruno, S., Pierri, F., Miano, M., Raggi, F., Farruggia, P., Mecucci, C., Crescenzi, B., Naim, V., et al. (2020). The passage from bone marrow niche to bloodstream triggers the metabolic impairment in Fanconi Anemia mononuclear cells. Redox Biol. *36*, 101618. https://doi.org/10.1016/j.redox.2020.101618.

10. Mombled, M., Rodriguez, L., Avalon, M., Duchez, P., Vlaski-Lafarge, M., Debeissat, C., Pérard, B., Sawai, K.M., Pasquet, J.M., Bijou, F., et al. (2020). Characteristics of cells with engraftment capacity within CD34+ cell population upon G-CSF and Plerixafor mobilization. Leukemia *34*, 3370–3381. https://doi.org/10.1038/s41375-020-0982-y.

11. Morgan, R.A., Gray, D., Lomova, A., and Kohn, D.B. (2017). Hematopoietic Stem Cell Gene Therapy: Progress and Lessons Learned. Cell Stem Cell *21*, 574–590. https://doi.org/10.1016/j.stem.2017.10.010.

12. Zonari, E., Desantis, G., Petrillo, C., Boccalatte, F.E., Lidonnici, M.R., Kajaste-Rudnitski, A., Aiuti, A., Ferrari, G., Naldini, L., and Gentner, B. (2017). Efficient Ex Vivo Engineering and Expansion of Highly Purified Human Hematopoietic Stem and Progenitor Cell Populations for Gene Therapy. Stem Cell Rep. *8*, 977–990. https://doi.org/10.1016/j.stemcr.2017.02.010.

13. Cannon, P., Asokan, A., Czechowicz, A., Hammond, P., Kohn, D.B., Lieber, A., Malik, P., Marks, P., Porteus, M., Verhoeyen, E., et al. (2021). Safe and Effective In Vivo Targeting and Gene Editing in Hematopoietic Stem Cells: Strategies for Accelerating Development. Hum. Gene Ther. *32*, 31–42. https://doi.org/10.1089/hum.2020.263.

14. Berraondo, P., Martini, P.G.V., Avila, M.A., and Fontanellas, A. (2019). Messenger RNA therapy for rare genetic metabolic diseases. Gut *68*, 1323–1330. https://doi.org/10.1136/gutjnl-2019-318269.

15. Breda, L., Papp, T.E., Triebwasser, M.P., Yadegari, A., Fedorky, M.T., Tanaka, N., Abdulmalik, O., Pavani, G., Wang, Y., Grupp, S.A., et al. (2023). In vivo hematopoietic stem cell modification by mRNA delivery. Science *381*, 436–443. https://doi.org/10.1126/science.ade6967.

16. Yu, X., Xu, T., Shi, H., Hong, J., Jin, X., Cao, L., Wang, J., Lin, Y., Pan, Z., Wang, S., et al. (2023). Cartilage-targeting mRNA-lipid nanoparticles rescue perifocal apoptotic

chondrocytes for integrative cartilage repair. Chem. Eng. J. *465*, 142841. https://doi.org/10.1016/j.cej.2023.142841.

17. Herrera-Barrera, M., Ryals, R.C., Gautam, M., Jozic, A., Landry, M., Korzun, T., Gupta, M., Acosta, C., Stoddard, J., Reynaga, R., et al. (2023). Peptide-guided lipid nanoparticles deliver mRNA to the neural retina of rodents and nonhuman primates. Sci. Adv. *9*, eadd4623. https://doi.org/10.1126/sciadv.add4623.

18. Li, B., Manan, R.S., Liang, S.Q., Gordon, A., Jiang, A., Varley, A., Gao, G., Langer, R., Xue, W., and Anderson, D. (2023). Combinatorial design of nanoparticles for pulmonary mRNA delivery and genome editing. Nat. Biotechnol. *41*, 1410–1415. https://doi.org/10.1038/s41587-023-01679-x.

19. Huayamares, S.G., Lokugamage, M.P., Rab, R., Da Silva Sanchez, A.J., Kim, H., Radmand, A., Loughrey, D., Lian, L., Hou, Y., Achyut, B.R., et al. (2023). High-throughput screens identify a lipid nanoparticle that preferentially delivers mRNA to human tumors in vivo. J. Contr. Release *357*, 394–403. https://doi.org/10.1016/j.jconrel.2023.04.005.

20. Alvarez, D., Masse-Ranson, G., Sedimbi, S.K., Wisti, P., Rodriguez, L., Santana, J., Manning, T., Towner, T., Geilich, B., Mihai, C., et al. (2022). Functional mRNA delivery to hematopoietic stem and progenitor cells in vivo. Preprint at bioRxiv. https://doi.org/10.1101/2022.12.15.520650.

21. Garaycoechea, J.I., and Patel, K.J. (2014). Why does the bone marrow fail in Fanconi anemia? Blood *123*, 26–34. https://doi.org/10.1182/blood-2013-09-427740.

22. Madisen, L., Zwingman, T.A., Sunkin, S.M., Oh, S.W., Zariwala, H.A., Gu, H., Ng, L.L., Palmiter, R.D., Hawrylycz, M.J., Jones, A.R., et al. (2010). A robust and high-throughput Cre reporting and characterization system for the whole mouse brain. Nat. Neurosci. *13*, 133–140. https://doi.org/10.1038/nn.2467.

23. Melamed, J.R., Hajj, K.A., Chaudhary, N., Strelkova, D., Arral, M.L., Pardi, N., Alameh, M.-G., Miller, J.B., Farbiak, L., Siegwart, D.J., et al. (2022). Lipid nanoparticle chemistry determines how nucleoside base modifications alter mRNA delivery. J. Contr. Release *341*, 206–214. https://doi.org/10.1016/j.jconrel.2021.11.022.

24. Chen, J., Xu, Y., Zhou, M., Xu, S., Varley, A.J., Golubovic, A., Lu, R.X.Z., Wang, K.C., Yeganeh, M., Vosoughi, D., and Li, B. (2023). Combinatorial design of ionizable lipid nanoparticles for muscle-selective mRNA delivery with minimized off-target effects. Proc. Natl. Acad. Sci. USA *120*, e2309472120. https://doi.org/10.1073/pnas.2309472120.

25. Dilliard, S.A., and Siegwart, D.J. (2023). Passive, active and endogenous organ-targeted lipid and polymer nanoparticles for delivery of genetic drugs. Nat. Rev. Mater. *8*, 282–300. https://doi.org/10.1038/s41578-022-00529-7.

26. Suzuki, H., Zuo, Y., Wang, J., Zhang, M.Q., Malhotra, A., and Mayeda, A. (2006). Characterization of RNase R-digested cellular RNA source that consists of lariat and circular RNAs from pre-mRNA splicing. Nucleic Acids Res. *34*, e63. https://doi.org/10.1093/nar/gkl151.

27. Wang, C., and Liu, H. (2022). Factors influencing degradation kinetics of mRNAs and half-lives of microRNAs, circRNAs, lncRNAs in blood in vitro using quantitative PCR. Sci. Rep. *12*, 7259. https://doi.org/10.1038/s41598-022-11339-w.

28. Wesselhoeft, R.A., Kowalski, P.S., and Anderson, D.G. (2018). Engineering circular RNA for potent and stable translation in eukaryotic cells. Nat. Commun. *9*, 2629. https://doi.org/10.1038/s41467-018-05096-6.

29. Walter, D., Lier, A., Geiselhart, A., Thalheimer, F.B., Huntscha, S., Sobotta, M.C., Moehrle, B., Brocks, D., Bayindir, I., Kaschutnig, P., et al. (2015). Exit from dormancy provokes DNA-damage-induced attrition in haematopoietic stem cells. Nature *520*, 549–552. https://doi.org/10.1038/nature14131.

30. Ceccaldi, R., Parmar, K., Mouly, E., Delord, M., Kim, J.M., Regairaz, M., Pla, M., Vasquez, N., Zhang, Q.S., Pondarre, C., et al. (2012). Bone marrow failure in Fanconi anemia is triggered by an exacerbated p53/p21 DNA damage response that impairs hematopoietic stem and progenitor cells. Cell Stem Cell *11*, 36–49. https://doi.org/10.1016/j.stem.2012.05.013.

31. Rodríguez, A., Zhang, K., Färkkilä, A., Filiatrault, J., Yang, C., Velázquez, M., Furutani, E., Goldman, D.C., García de Teresa, B., Garza-Mayén, G., et al. (2021). MYC Promotes Bone Marrow Stem Cell Dysfunction in Fanconi Anemia. Cell Stem Cell *28*, 33–47.e38. https://doi.org/10.1016/j.stem.2020.09.004.

32. Alameh, M.G., Tombácz, I., Bettini, E., Lederer, K., Sittplangkoon, C., Wilmore, J.R., Gaudette, B.T., Soliman, O.Y., Pine, M., Hicks, P., et al. (2021). Lipid nanoparticles enhance the efficacy of mRNA and protein subunit vaccines by inducing robust T follicular helper cell and humoral responses. Immunity *54*, 2877–2892.e2877. https://doi.org/10.1016/j.immuni.2021.11.001.

33. Ndeupen, S., Qin, Z., Jacobsen, S., Bouteau, A., Estanbouli, H., and Igyártó, B.Z. (2021). The mRNA-LNP platform's lipid nanoparticle component used in preclinical vaccine studies is highly inflammatory. iScience *24*, 103479. https://doi.org/10.1016/j.isci.2021.103479.

34. Gentner, B., and Naldini, L. (2019). In Vivo Selection for Gene-Corrected HSPCs Advances Gene Therapy for a Rare Stem Cell Disease. Cell Stem Cell *25*, 592–593. https://doi.org/10.1016/j.stem.2019.10.004.

35. Zhou, Y., He, Y., Xing, W., Zhang, P., Shi, H., Chen, S., Shi, J., Bai, J., Rhodes, S.D., Zhang, F., et al. (2017). An abnormal bone marrow microenvironment contributes to hematopoietic dysfunction in Fanconi anemia. Haematologica *102*, 1017–1027. https://doi.org/10.3324/haematol.2016.158717.

36. Lecourt, S., Vanneaux, V., Leblanc, T., Leroux, G., Ternaux, B., Benbunan, M., Chomienne, C., Baruchel, A., Marolleau, J.P., Gluckman, E., et al. (2010). Bone marrow microenvironment in fanconi anemia: a prospective functional study in a cohort of fanconi anemia patients. Stem Cell. Dev. *19*, 203–208. https://doi.org/10.1089/scd.2009.0062.

37. Li, Y., Chen, S., Yuan, J., Yang, Y., Li, J., Ma, J., Wu, X., Freund, M., Pollok, K., Hanenberg, H., et al. (2009). Mesenchymal stem/progenitor cells promote the reconstitution of exogenous hematopoietic stem cells in Fancg-/- mice in vivo. Blood *113*, 2342–2351. https://doi.org/10.1182/blood-2008-07-168138.

38. Shirley, J.L., de Jong, Y.P., Terhorst, C., and Herzog, R.W. (2020). Immune Responses to Viral Gene Therapy Vectors. Mol. Ther. *28*, 709–722. https://doi.org/10.1016/j.ymthe.2020.01.001.

39. Siegner, S.M., Ugalde, L., Clemens, A., Garcia-Garcia, L., Bueren, J.A., Rio, P., Karasu, M.E., and Corn, J.E. (2022). Adenine base editing efficiently restores the function of Fanconi anemia hematopoietic stem and progenitor cells. Nat. Commun. *13*, 6900. https://doi.org/10.1038/s41467-022-34479-z.

40. Li, C., Georgakopoulou, A., Mishra, A., Gil, S., Hawkins, R.D., Yannaki, E., and Lieber, A. (2021). In vivo HSPC gene therapy with base editors allows for efficient reactivation of fetal γ-globin in β-YAC mice. Blood Adv. *5*, 1122–1135. https://doi.org/10.1182/bloodadvances.2020003702.

41. Aliahmad, P., Miyake-Stoner, S.J., Geall, A.J., and Wang, N.S. (2023). Next generation self-replicating RNA vectors for vaccines and immunotherapies. Cancer Gene Ther. *30*, 785–793. https://doi.org/10.1038/s41417-022-00435-8.

42. Geall, A.J., Verma, A., Otten, G.R., Shaw, C.A., Hekele, A., Banerjee, K., Cu, Y., Beard, C.W., Brito, L.A., Krucker, T., et al. (2012). Nonviral delivery of self-amplifying RNA vaccines. Proc. Natl. Acad. Sci. USA *109*, 14604–14609. https://doi.org/10.1073/pnas.1209367109.

43. Pepini, T., Pulichino, A.M., Carsillo, T., Carlson, A.L., Sari-Sarraf, F., Ramsauer, K., Debasitis, J.C., Maruggi, G., Otten, G.R., Geall, A.J., et al. (2017). Induction of an IFN-Mediated Antiviral Response by a Self-Amplifying RNA Vaccine: Implications for Vaccine Design. J. Immunol. *198*, 4012–4024. https://doi.org/10.4049/jimmunol.1601877.

44. Maertens, G.N., Engelman, A.N., and Cherepanov, P. (2022). Structure and function of retroviral integrase. Nat. Rev. Microbiol. *20*, 20–34. https://doi.org/10.1038/s41579-021-00586-9.

45. Annoni, A., Gregori, S., Naldini, L., and Cantore, A. (2019). Modulation of immune responses in lentiviral vector-mediated gene transfer. Cell. Immunol. *342*, 103802. https://doi.org/10.1016/j.cellimm.2018.04.012.

46. Chen, S., Zaifman, J., Kulkarni, J.A., Zhigaltsev, I.V., Tam, Y.K., Ciufolini, M.A., Tam, Y.Y.C., and Cullis, P.R. (2018). Dexamethasone prodrugs as potent suppressors of the immunostimulatory effects of lipid nanoparticle formulations of nucleic acids. J. Contr. Release *286*, 46–54. https://doi.org/10.1016/j.jconrel.2018.07.026.

47. Chen, M., Tomkins, D.J., Auerbach, W., McKerlie, C., Youssoufian, H., Liu, L., Gan, O., Carreau, M., Auerbach, A., Groves, T., et al. (1996). Inactivation of Fac in mice produces inducible chromosomal instability and reduced fertility reminiscent of Fanconi anaemia. Nat. Genet. *12*, 448–451. https://doi.org/10.1038/ng0496-448.

48. Wilkinson, A.C., Ishida, R., Kikuchi, M., Sudo, K., Morita, M., Crisostomo, R.V., Yamamoto, R., Loh, K.M., Nakamura, Y., Watanabe, M., et al. (2019). Long-term ex vivo haematopoietic-stem-cell expansion allows nonconditioned transplantation. Nature *571*, 117–121. https://doi.org/10.1038/s41586-019-1244-x.

OMTN, Volume *36*

Supplemental information

Restoring hematopoietic stem and progenitor cell function in *Fancc*$^{-/-}$ mice by *in situ* delivery of RNA lipid nanoparticles

Omar Banda, Sarah E. Adams, Linah Omer, Seul K. Jung, Hooda Said, Theerapat Phoka, Ying Tam, Drew Weissman, Stefano Rivella, Mohamad-Gabriel Alameh, and Peter Kurre

Table S1 – List of Materials

REAGENT or RESOURCE	SOURCE	IDENTIFIER
Antibodies		
Alexa Fluor® 700 anti-CD48 (HM48-1)	Biolegend	Cat# 103426, RRID: AB_10612755
APC/Cyanine7 anti-Sca-1 (D7)	Biolegend	Cat# 108126, RRID: AB_10645327
Brilliant Violet 650™ anti-CD45.2 (104)	Biolegend	Cat# 109836, RRID: AB_2563065
Brilliant Violet 711™ anti-CD150 (TC15-12F12.2)	Biolegend	Cat# 115941, RRID: AB_2629660
BUV395 Anti-Mouse CD117 (2B8)	BD Horizon™	Cat# 564011, RRID: AB_2738541
FITC anti-mouse Lineage Cocktail with Isotype Ctrl	Biolegend	Cat# 133302, AB_10697030
APC/Cyanine7 anti-mouse CD45.2 Antibody	Biolegend	Cat# 109824, RRID: AB_830789
Alexa Fluor® 700 anti-mouse CD31 Antibody	Biolegend	Cat# 102444, RRID: AB_2832289
CD51 antibody | RMV-7	Bio-Rad	Cat# MCA2461, RRID: AB_931725
FITC anti-mouse TER-119 Antibody	Biolegend	Cat# 116206, RRID: AB_313707
Pacific Blue™ anti-mouse Ly-6A/E (Sca-1) Antibody	Biolegend	Cat# 108120, RRID: AB_493273
PE/Cyanine5 anti-mouse CD135 Antibody	Biolegend	Cat# 135312, RRID: AB_2263031
PE/Cyanine7 anti-mouse CD45.1 Antibody	Biolegend	Cat# 110730, RRID: AB_1134168
APC/Cyanine7 anti-mouse CD117 (c-kit) Antibody	Biolegend	Cat# 105826, RRID: AB_1626278
Chemicals, Peptides, and Recombinant Proteins		
DAPI (4',6-Diamidino-2-Phenylindole, Dilactate)	Biolegend	Cat# 422801
Recombinant murine thrombopoietin	Peprotech	Cat# 315-14
Recombinant murine stem cell factor	Peprotech	Cat# 250-03
Insulin–transferrin–selenium–ethanolamine	Gibco	Cat# 51500-056

HEPES	Gibco	Cat# 15630-080
Polyvinyl alcohol	Sigma	Cat# P8136
10X RBC lysis buffer	eBioscience™	Cat# 00-4300-54
Fibronectin human plasma	Sigma Aldrich	Cat# F0895
Critical Commercial Assays		
EasySep™ Mouse Hematopoietic Progenitor Cell Isolation Kit	StemCell Technologies	Cat# 19856
Experimental Models: Organisms/Strain		
Mouse: C57BL/6-Ly5.2 Fancc(+/-)	Dr. Manuel Buchwald's Laboratory	https://doi.org/10.1038/ng0496-448
Mouse: B6.SJL-*Ptprc*^{a} *Pepc*^{b}/BoyJ	Jackson laboratories	https://www.jax.org/strain/002014
Software and Algorithms		
Prism 9	GraphPad	https://www.graphpad.com/scientific-software/prism/
Matlab (R2021a)	Mathworks	https://www.mathworks.com/

Table S2 – LNP Formulation Method

Figure	AcuitasTX	In-house
1	**a-c**	**d-f**
2	✓	
3	✓	
4		✓
5	**a-d**	**e-h**
6		✓
7		✓
S1		
S2		✓
S3		✓
S4		✓
S5		✓
S6		✓
S7	✓	
S8	**c-e**	**a, b, f**

Figure S1

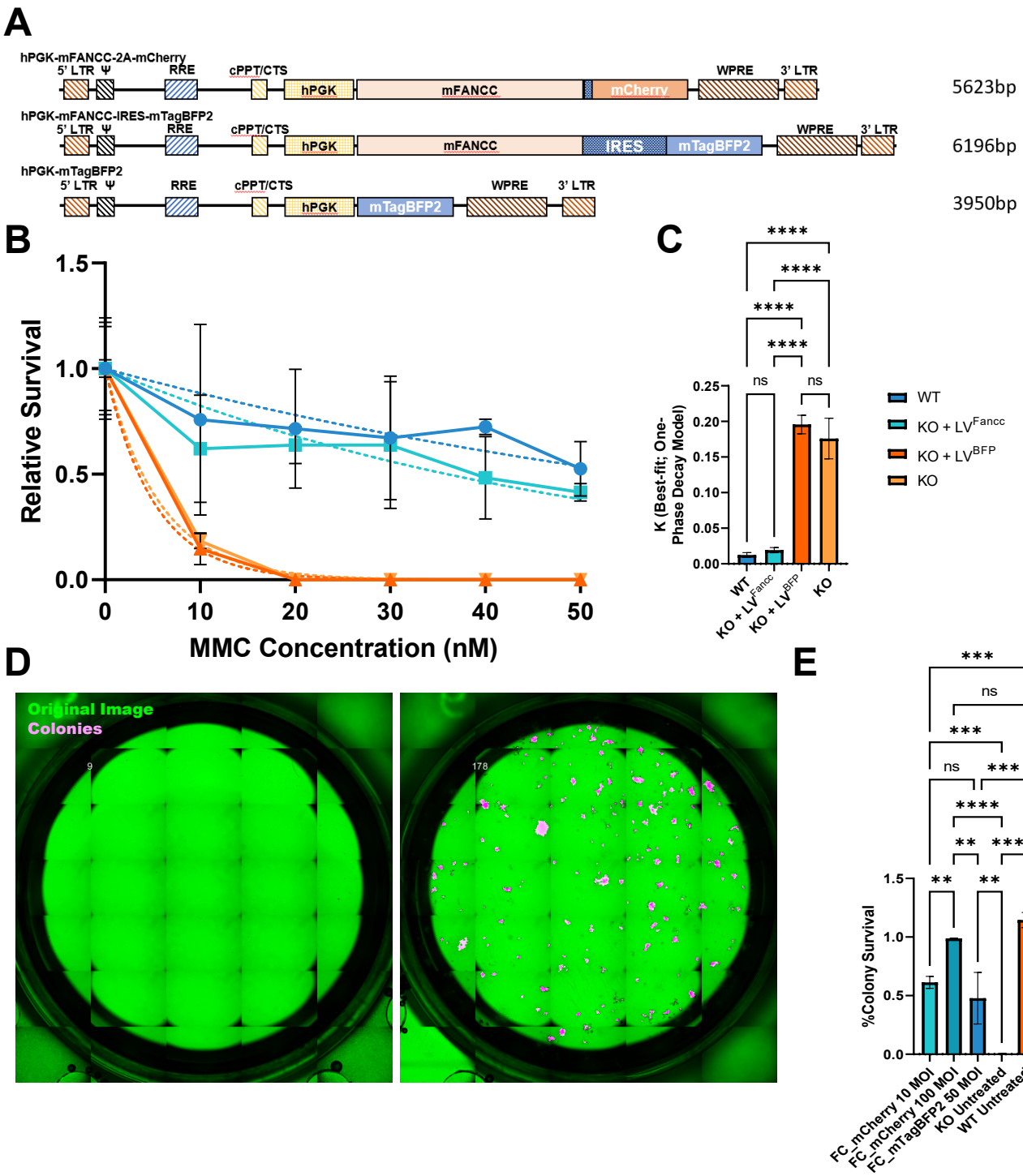

Figure S1 - Lentiviral Transduction of Fancc$^{(-/-)}$ mice to restore MMC tolerance. (A) The murine Fancc gene was cloned into a 3rd generation lentiviral transfer plasmid under control of the human PGK promoter. (B-C) Plot of the relative colony survival of Fancc$^{(-/-)}$ or wild-type KSL populations in methylcellulose media with or without 0-50nM MMC. Data are fit with exponential decay model constrained to full survival at 0nM MMC and plateau at 0% relative survival. (D) Representative images of 30nM CFU assay (green) with detected colonies (magenta) overlayed for non-transduced Fancc$^{(-/-)}$ cells (left) and LVFancc-transduced Fancc$^{(-/-)}$ cells (right). (E) Colony survival under various transduction schemes.

Figure S2

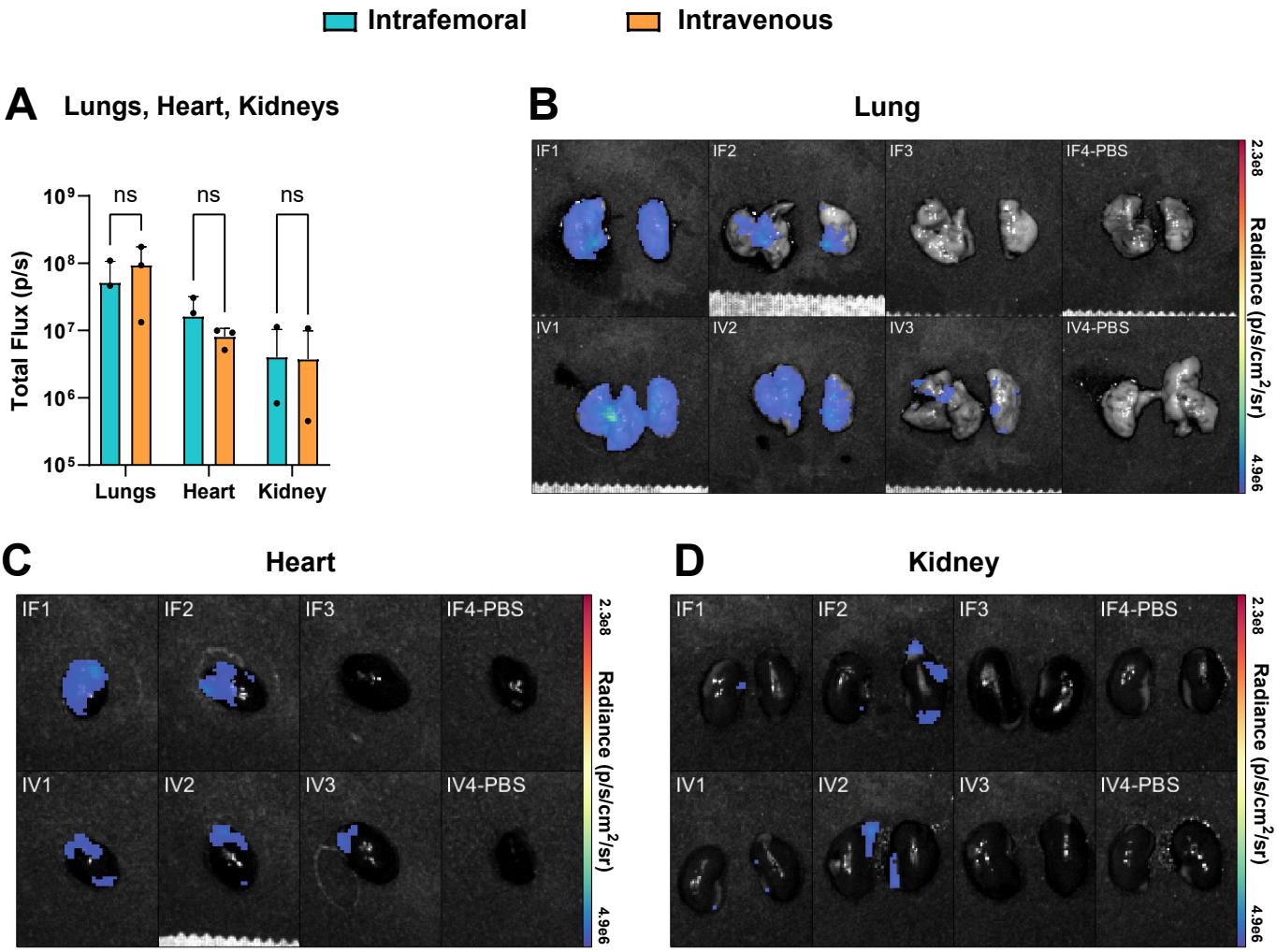

Figure S2 - LNP^{LFluc} expression in lungs, heart, and kidneys after intrafemoral or intravenous delivery. (A) The total luminescent flux measured 10 minutes after D-luciferin administration in LNP^{LFluc} treated mice is shown. (B-D) Heatmaps of radiance in organs corresponding to those in (A), reveal the distribution of radiance displayed as an overlay on reflected light images of the organs.

Figure S3

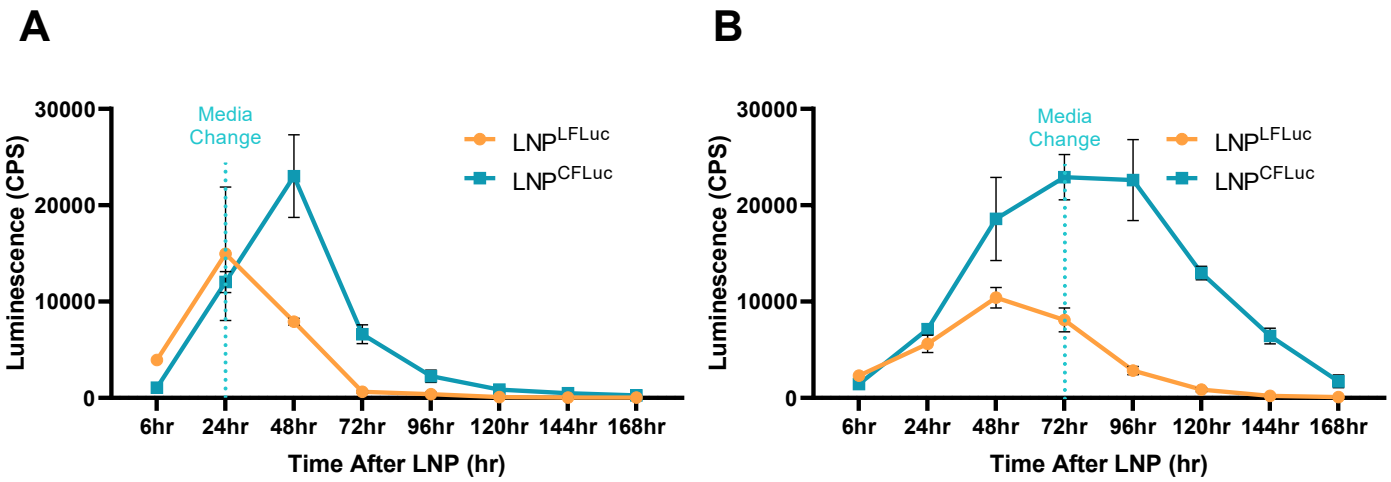

Figure S3 - Increased exposure time of LNPs increases total expression and peak expression time.
(A,B) Time-series plots of luminescence as a function of time post exposure to either linear or circular Luciferase mRNA delivered with LNPs in MEFs. Excess extracellular LNPs were removed from cells either 24 hours (A) or 72 hours (B) post-exposure by a media change.

Figure S4

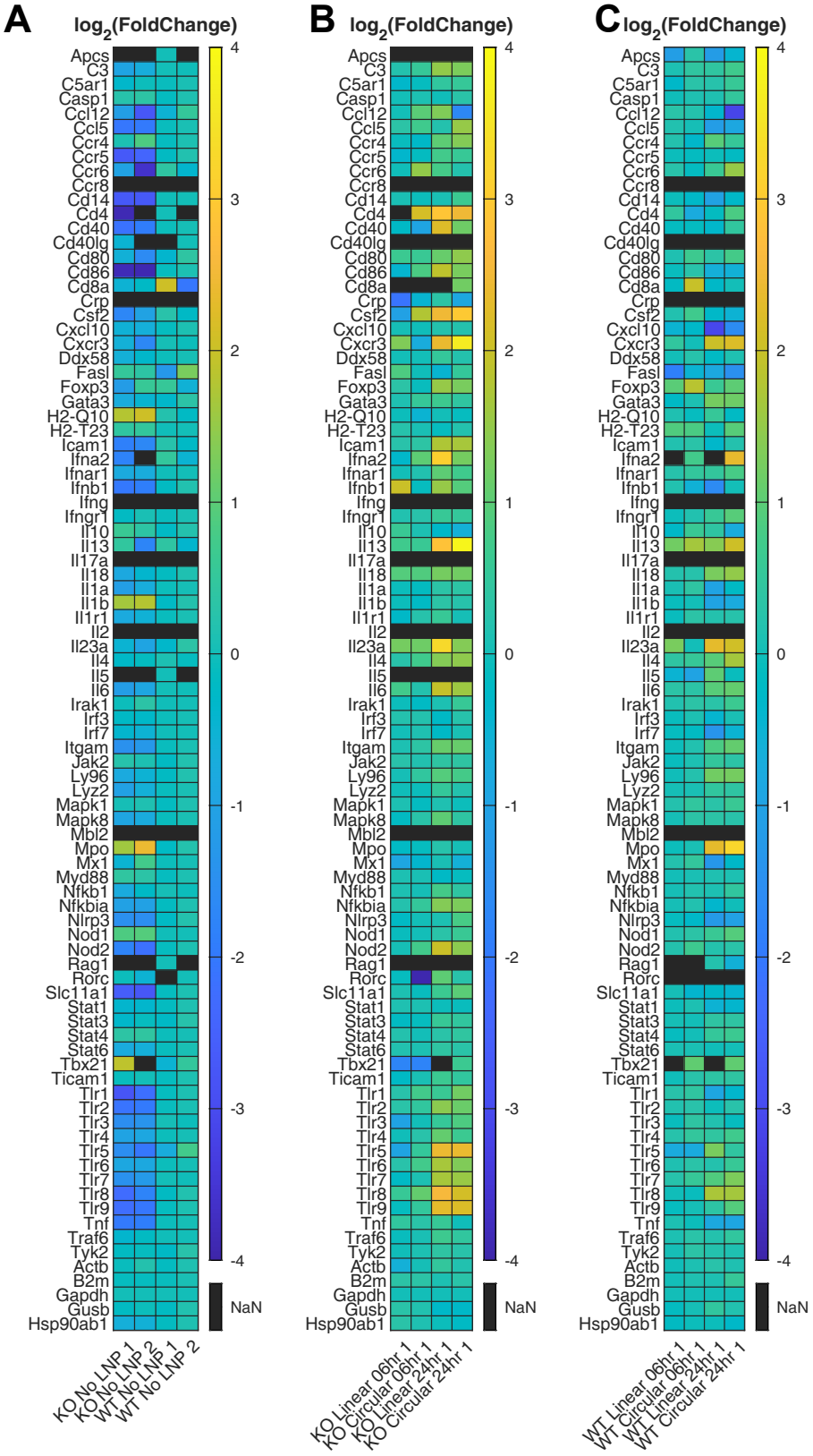

Figure S4 - qRT-PCR Array Screening of LNP-treated *ex vivo* expanded wildtype and Fancc$^{(-/-)}$ LT-HSC. *Ex vivo* expanded LT-HSCs were treated with either LNP^{LFancc} or LNP^{CFancc} for 6 or 24 hours and RNA content was analyzed by qRT-PCR. (A) A heatmap of relative transcript concentrations highlighting baseline differences between Fancc$^{(-/-)}$ and wildtype cells. Values are expressed as the binary log of fold change difference from the mean value of the wildtype cells. Additional heatmaps highlighting differences in relative transcript concentrations of the mutant cells (B) or wildtype cells(C) after treatment with Fancc mRNA from the respective mean of untreated controls. All fold change values are calculated as the relative concentration difference to the untreated control after normalization to Gapdh.

Figure S5

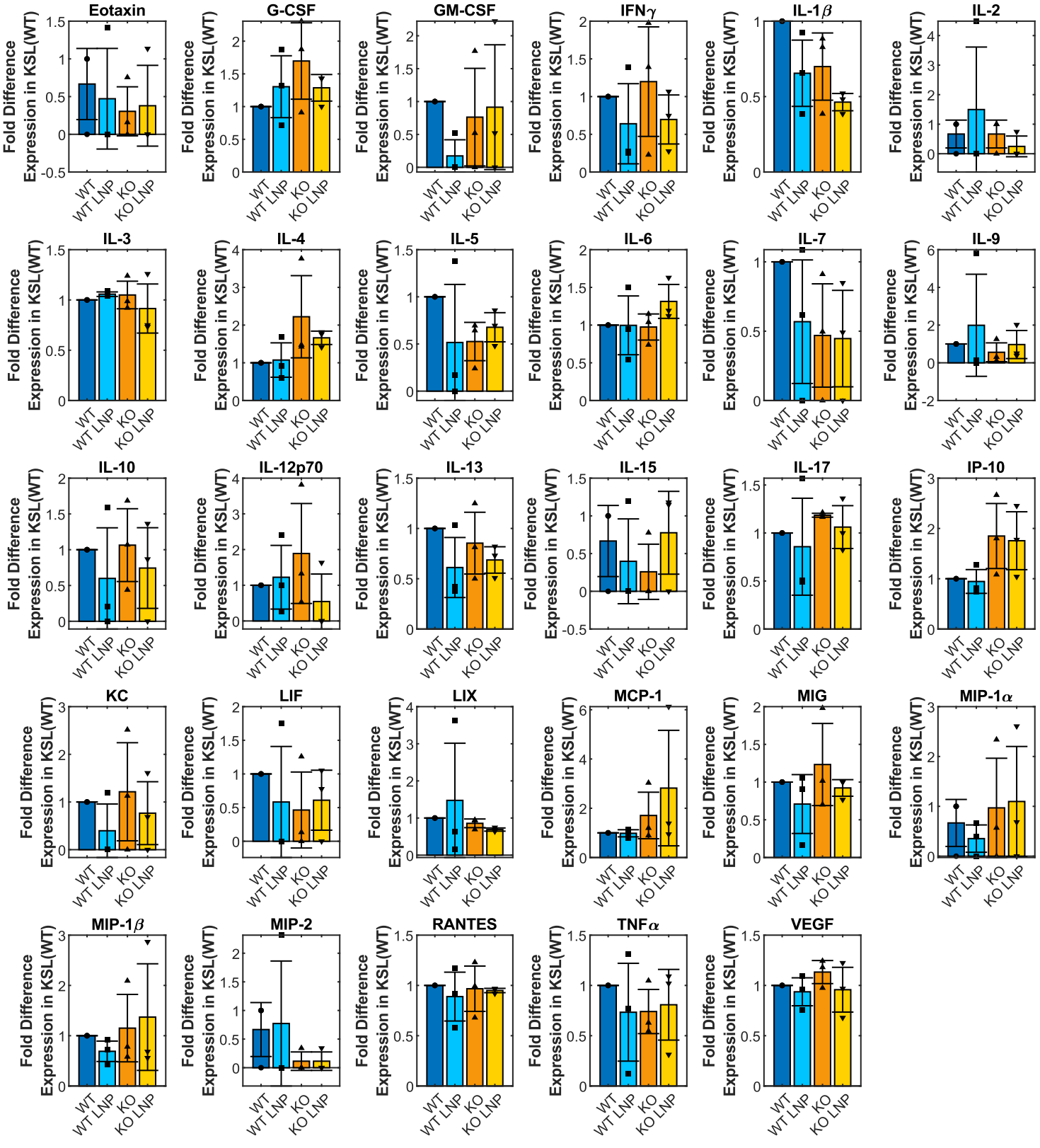

Figure S5 – Immune cytokine expression of KSL populations after LNP^{CFancc} exposure. Cytokine expression in KSL media supernatant was measured by Mouse Cytokine 32-Plex Discovery Assay (Eve Technologies Corporation) after LNP^{CFancc} treatment and a 24hr incubation period. Each data point reflects pooled supernatants from an individual cohort. Values are displayed as the fold difference expression measured in the untreated wildtype from the respective cohort.

Figure S6

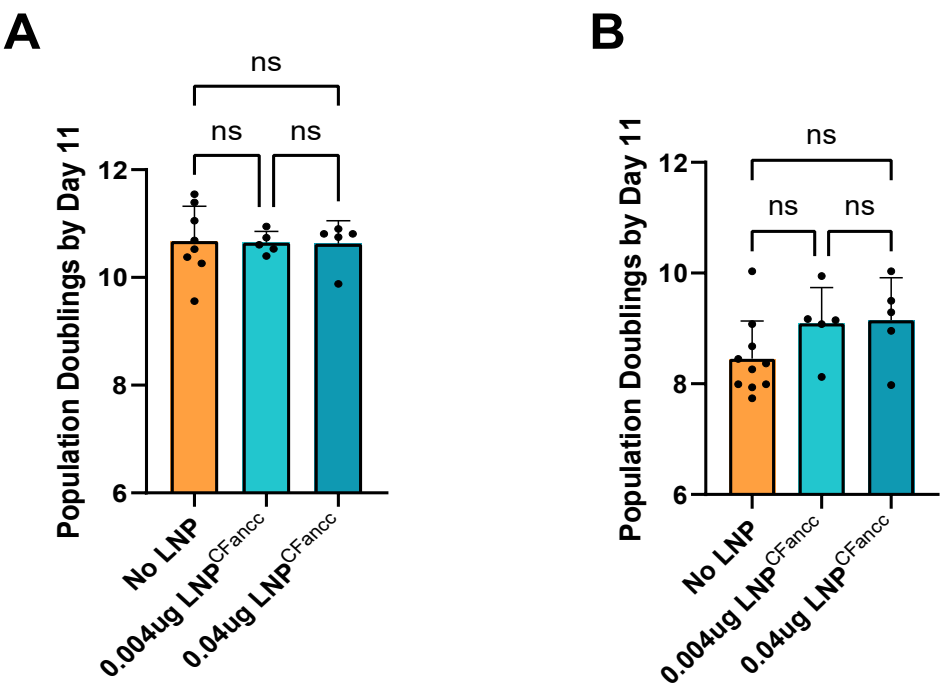

Figure S6 – Impact of a single dose of LNP^{CFancc} on proliferation of *ex vivo* expanded LT-HSCs.

LT-HSCs sorted from freshly isolated bone marrow were treated with a single dose (0.004ug or 0.04ug RNA) of LNP^{CFancc} and expanded over 11 days. Cells were counted after 11 days of culture to determine the total number of population doublings in (A) wild-type and (B) Fancc(-/-) populations.

Figure S7

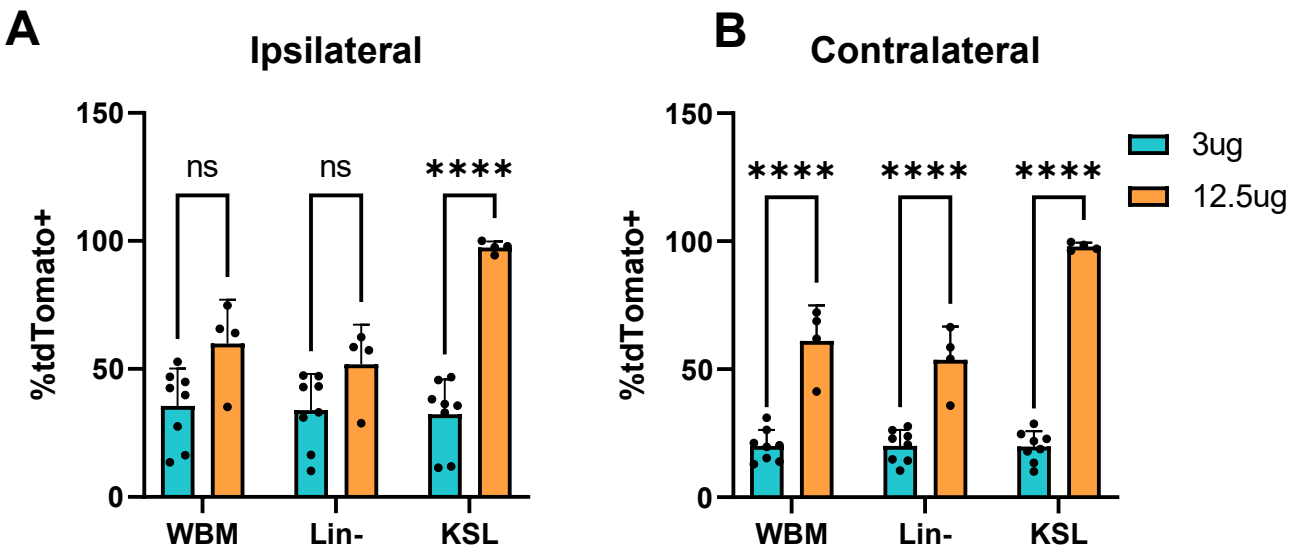

Figure S7 - tdTomato expression after LNP^{Cre} Treatment is correlated to LNP dose. Displayed are positivity rates of tdTomato in bone marrow populations after either 3ug or 12.5ug doses of LNP^{Cre} administered intrafemorally measured in (A) ipsilateral, or (B) contralateral femurs.

Figure S8

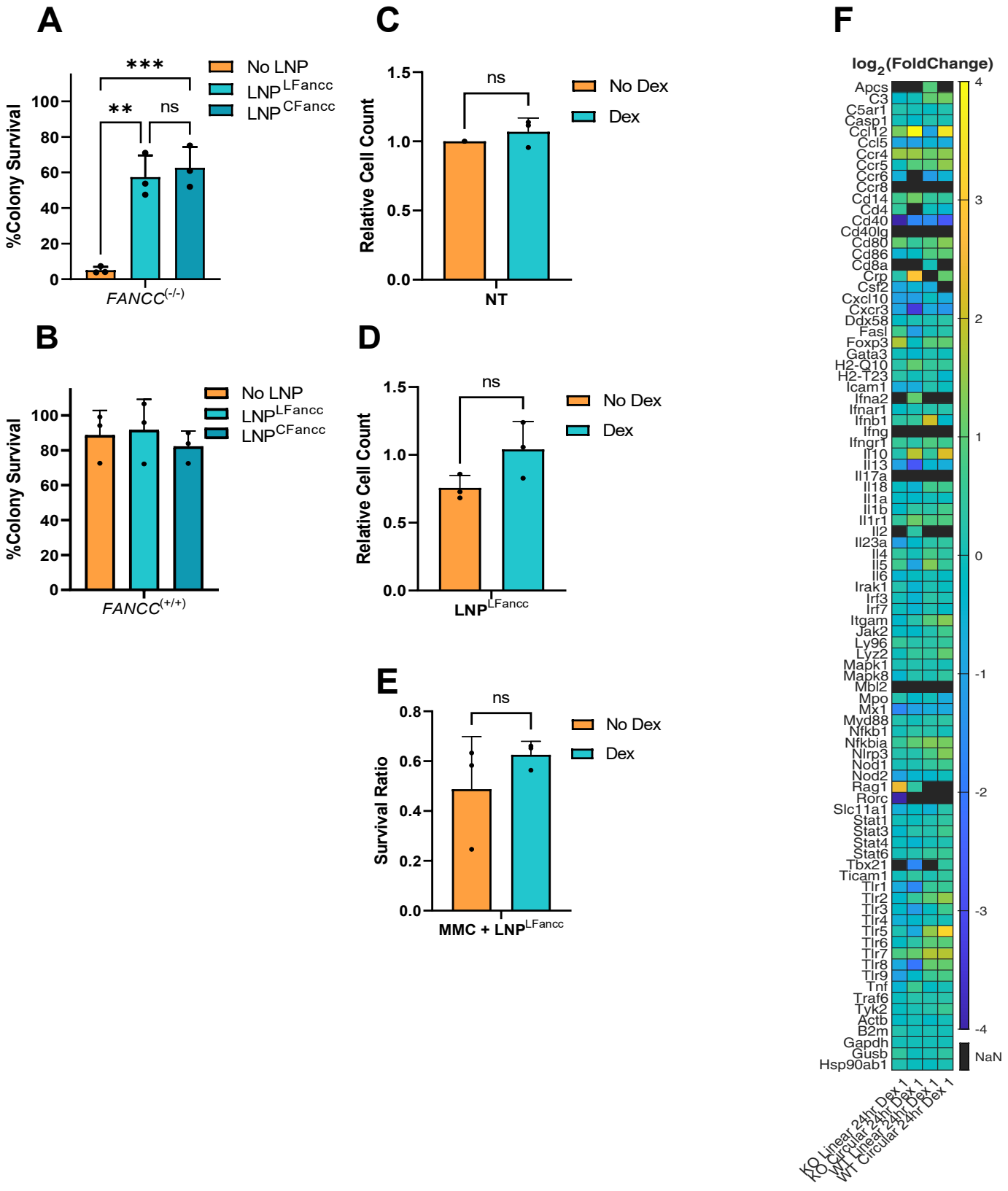

Figure S8 - Addition of dexamethasone to BM populations in vitro does not affect conferral of Fancc functionality. (A,B) *Ex vivo* expanded HSCs plated into CFU assay as in Figure 1 after exposure to 100nM dexamethasone during LNP treatment and MMC exposure. No impact of dexamethasone on colony survival was observed. (C-E) Similarly, no impact is measured on in vitro proliferation as a function of cell counts or in the survival rate after MMC exposure in Lin- populations. (F) Screening by qRT-PCR highlighting differences in immune marker expression when treated with LNPs in the presence of dexamethasone. All values are normalized to the respective LNP treated cells without dexamethasone.